

1  
2  
3  
4  
5  
6  
7  
8  
9  
10  
11  
12  
13  
14  
15  
16  
17  
18  
19  
20  
21  
22  
23  
24  
25  
26  
27  
28  
29  
30  
31  
32  
33  
34  
35  
36  
37  
38  
39  
40  
41  
42  
43  
44  
45  
46  
47  
48  
49  
50  
51  
52  
53  
54  
55  
56  
57  
58  
59  
60  
61  
62  
63  
64  
65

## Surface transport in the Northeastern Adriatic Sea from FSLE analysis of HF radar measurements

Maristella Berta<sup>a,b,\*</sup>, Laura Ursella<sup>a</sup>, Francesco Nencioli<sup>c</sup>, Andrea M. Doglioli<sup>c</sup>,  
Anne A. Petrenko<sup>c</sup>, Simone Cosoli<sup>a</sup>

<sup>a</sup>*Istituto Nazionale di Oceanografia e di Geofisica sperimentale - OGS, Trieste, Italy*

<sup>b</sup>*University of Trieste, Trieste, Italy*

<sup>c</sup>*Aix-Marseille University, Mediterranean Institute of Oceanography (MIO), 13288,  
Marseille, Cedex 9, France ; Université du Sud Toulon-Var, CNRS-INSU/IRD UM 110*

---

### Abstract

This study focuses on the surface transport in the Northeastern Adriatic Sea and the related hydrodynamic connectivity with the Gulf of Trieste (GoT) under [calm or typical wind conditions](#): Bora (from the NE) and Sirocco (from the SE). The surface transport in the area has been investigated by evaluating the Finite-Size Lyapunov Exponents (FSLE) on the current field measured by the High Frequency (HF) coastal radar network. FSLE allow to estimate Lagrangian Coherent Structures (LCSs), which provide information on the transport patterns associated with the flow and identify regions characterized by different dynamics. This work includes the development and set up of the FSLE algorithm applied for the first time to the specific Adriatic area considered. The FSLE analysis during calm wind reveals an attractive LCS crossing the GoT entrance, marking the convergence between the Northern Adriatic and the outflowing gulf waters. During Bora episodes this attractive LCS is displaced westward with respect to the calm wind case, indicating that Bora drives an extended coherent outflow from the GoT. [On the other hand, Sirocco wind piles up the water along the northern end of the basin. In this area an attractive LCS is found, extending mainly in SW-NE direction. The sirocco-induced inflow of Adriatic waters in](#)

---

\*CNR-ISMAR. Forte Santa Teresa, Pozzuolo di Lerici, 19032 (SP). Italy. Tel: (+39)0187-978316

*Email address:* [maristella.bera@sp.ismar.cnr.it](mailto:maristella.bera@sp.ismar.cnr.it) (Maristella Berta)

1  
2  
3  
4  
5  
6  
7  
8  
9 the GoT is mainly driven along its northern (Italian) side, as evidenced by the  
10 orientation of the LCS. Under Sirocco condition, as in Bora case, there is no  
11 barrier in front of the gulf. No relevant LCSs are observed in the southern radar  
12 coverage area except for Bora cases, when a repulsive LCS develops in front of  
13 the Istrian coast separating water masses to the North and the South of it.  
14  
15

16 *Keywords:* Adriatic Sea, Trieste Gulf, radar, surface transport, FSLE, LCS  
17  
18

---

19  
20 **1. Introduction**  
21

22 The Adriatic Sea is a basin of the Eastern Mediterranean Sea enclosed be-  
23 tween the Italian and the Balkan peninsula, and it separates respectively the  
24 Apennine mountains from the Dinaric Alps (Figure 1). It extends in the NW-  
25 SE direction and communicates with the Ionian Sea through the Otranto Strait,  
26 located at its southern end. The mean surface circulation of the Adriatic Sea  
27 is characterized by a northwestward flow along the Balkan coast, known as the  
28 Eastern Adriatic Current (EAC), and a southeastward flow along the Italian  
29 coast, called Western Adriatic Current (WAC) [Artegiani et al., 1997b; Zore,  
30 1956]. The EAC-WAC system results in a basin-wide cyclonic circulation in  
31 which three cyclonic gyres are embedded at the southern, middle and northern  
32 part of the Adriatic Sea, respectively [Artegiani et al., 1997a; Malanotte-Rizzoli  
33 and Bergamasco, 1983]. Observations of water mass properties and currents ev-  
34 idence that the Northern Adriatic circulation is strongly influenced by the winds  
35 over the Adriatic area [Poulain et al., 2001]. Due to its geographical orientation  
36 with respect to the surrounding orography (Apennines and Dinaric Alps) it is  
37 particularly affected by Bora and Sirocco winds [Orlić et al., 1994].  
38  
39

40 The Bora is a northeasterly cold and dry katabatic wind, with the most  
41 severe manifestations occurring typically during winter [Yoshino, 1976]. The  
42 Sirocco blows from S-SE and by crossing the Mediterranean Sea it gets warm  
43 and humid. Unlike the Bora, which is characterized by a gusty nature, it keeps  
44 more homogeneous spatial characteristics over the Adriatic Sea [Ferrarese et al.,  
45 2008].  
46  
47  
48  
49  
50  
51  
52  
53  
54  
55  
56  
57  
58  
59  
60  
61  
62  
63  
64  
65

1  
2  
3  
4  
5  
6  
7  
8  
9  
10  
11  
12  
13  
14  
15  
16  
17  
18  
19  
20  
21  
22  
23  
24  
25  
26  
27  
28  
29  
30  
31  
32  
33  
34  
35  
36  
37  
38  
39  
40  
41  
42  
43  
44  
45  
46  
47  
48  
49  
50  
51  
52  
53  
54  
55  
56  
57  
58  
59  
60  
61  
62  
63  
64  
65

24 In the Northern Adriatic area, the Bora drives several dynamical processes  
25 both at the surface and in the deeper layers. These include the dense water  
26 formation in the northern and central part, the latter compensated by strong  
27 upwelling along the eastern margin [Lazar et al., 2007; Orlić et al., 1992], and  
28 the intensification of the WAC [Ursella et al., 2006]. The most prominent Bora-  
29 induced feature is a double gyre circulation [Zore-Armanda and Gačić, 1987]  
30 developing as a consequence of the funneling of Bora to the North and the  
31 South of Istria (these paths are called “Bora corridors”) [Lazić and Tošić, 1998].  
32 This pattern has been identified both by drifters trajectories [Poulain, 2001] and  
33 by model simulations [Kuzmić et al., 2007; Jeffries and Lee, 2007]. On the other  
34 hand Sirocco enhances the EAC [Ursella et al., 2006] by piling up sea water  
35 along the Northern Adriatic coasts. Occasionally it can reverse the WAC along  
36 the Italian coastline, inducing a north-westward current particularly intense in  
37 the Northern part of the basin [Ferrarese et al., 2008; Kovačević et al., 2004].  
38 As a consequence, sea level rise is often observed in the region during Sirocco  
39 episodes [Orlić et al., 1994].

40 This study focuses on the northeastern area, which corresponds to the shal-  
41 low area of the basin and thus it is extremely sensitive to wind forcing and  
42 riverine inputs (Po, Tagliamento, Isonzo; Figure 1). For these reasons, surface  
43 currents in this part of the Adriatic Sea, have been continuously monitored by a  
44 coastal radar network in the framework of the NASCUM (North Adriatic Sur-  
45 face CUREnt Mapping) project. The surface currents in this area were analyzed  
46 by Mihanović et al. [2011] through the SOM (Self-Organizing Map) technique to  
47 identify the typical patterns developing for different wind conditions, with par-  
48 ticular emphasis on those associated with the prevailing wind regimes of Bora  
49 and Sirocco. The detected current patterns were indeed characterized by the  
50 expected circulation response, but, at the same time, they also evidenced new  
51 sub-mesoscale features never reported in previous studies.

52 The present study will focus on the eastern part of the Northern Adriatic,  
53 aiming in particular at investigating the surface transport and the related hy-  
54 drodynamic connectivity associated with the surface circulation between the

1  
2  
3  
4  
5  
6  
7  
8  
9  
55 Gulf of Trieste (GoT) and the Northern Adriatic Sea under the typical wind  
10 conditions. The GoT is defined as the region of the Adriatic Sea North-East of  
11 the ideal line connecting Savudrija and Grado (Figure 1). According to Malačić  
12 and Petelin [2001] and Bogunović and Malačić [2009] the circulation in the GoT  
13 is driven by the EAC intrusion at intermediate depth along the southern side of  
14 the gulf. This induces GoT waters to follow the gulf coastline with a cyclonic  
15 pattern and then exit along the Italian margin. At the same time, a transversal  
16 outflow current develops at the surface crossing the GoT entrance from SE to  
17 NW [Malačić and Petelin, 2009].  
18  
19  
20  
21  
22

23 The surface transport in the area will be investigated through the Finite-  
24 Size Lyapunov Exponent (FSLE) technique. This method allows to identify  
25 Lagrangian Coherent Structures (LCSs) on the basis of the relative dispersion  
26 between initially close particles. LCSs provide information on the transport  
27 patterns associated with the flow and they allow to identify regions character-  
28 ized by different dynamics [Ottino, 1989; d’Ovidio et al., 2004]. They indicate  
29 the directions along which water masses are advected by the flow; and, at the  
30 same time, the converging and diverging regions of the flow, since water masses  
31 are squeezed along attractive LCSs and stretched across repulsive ones. Finally,  
32 LCSs also represent transport barriers since they cannot be crossed by the ad-  
33 vected water masses. The FSLE method can be regarded as a complementary  
34 approach with respect to other Eulerian analysis usually applied to identify  
35 eddy’s core and to characterize mixing based on velocity field snapshots (such  
36 as vortex identification from eddy kinetic energy or Okubo-Weiss parameter).  
37 In fact FSLE maps depend on the spatio-temporal evolution of the velocity field  
38 and of its transport properties, and not only on the velocity configuration at a  
39 given scale and time [García-Olivares et al., 2007; d’Ovidio et al., 2009]. Since  
40 FSLE maps are computed through the integration of particle trajectories, they  
41 identify dynamical structures that organize the transport in a velocity field, with  
42 details below its original resolution and without any assumption on small scale  
43 dispersion features [Hernández-Carrasco et al., 2011]. This is possible because  
44 the integration of trajectories from an Eulerian velocity map to the next ones al-  
45  
46  
47  
48  
49  
50  
51  
52  
53  
54  
55  
56  
57  
58  
59  
60  
61  
62  
63  
64  
65

1  
2  
3  
4  
5  
6  
7  
8  
9 86 lows to extract the information contained in the flow field temporal dependence,  
10 87 that on the other hand is lost when looking at each velocity map independently.  
11  
12 88 Indeed, the trajectories of the synthetic particles advected in the surface current  
13 89 fields capture the smaller scale dynamics resulting from the variability of the  
14 90 mesoscale field.

15  
16 91 In the Adriatic Sea, the FSLE method has been first used by Haza et al.  
17 92 [2007] to identify LCSs from NCOM (Navy Coastal Ocean Model) currents.  
18 93 Being based on a numerical model output, the comparison between the drifter  
19 94 trajectories and the identified LCSs corroborated the potential of integrating  
20 95 predictive coastal models with the FSLE method. A subsequent work by Haza  
21 96 et al. [2008] investigated the relative dispersion for the whole Adriatic Sea based  
22 97 on the NCOM model currents. The study showed that tracer dispersion is  
23 98 mainly controlled by large-scale circulation rather than by local regimes. This  
24 99 is in agreement with other studies based on open ocean LCSs derived from  
25 100 satellite velocity fields [Lehahn et al., 2007; d’Ovidio et al., 2009]. Nonetheless,  
26 101 a recent study by Nencioli et al. [2011] has shown that smaller scale processes,  
27 102 not resolved by large scale model or satellite data, are fundamental for studying  
28 103 transport patterns in coastal areas.

29  
30  
31 104 In terms of small scale processes, HF radars have a clear advantage over  
32 105 large scale models and satellite surveying, in that velocities measured by HF  
33 106 radar include processes over a broader range of spatial and temporal scales  
34 107 (from the submesoscale to larger scale circulation). For this reason, radar ve-  
35 108 locities are particularly suited for the analysis of coastal LCSs. This has been  
36 109 confirmed by the study performed in the Ligurian Sea by Haza et al. [2010],  
37 110 in which LCSs identified from VHF WERA radar current fields [Gurgel et al.,  
38 111 1999] were compared with the trajectories of drifter clusters. Although the LCS  
39 112 theory assumes 2D non-divergent flows, it was found that the motion of the  
40 113 surface drifters followed the VHF radar derived transport barriers, in spite of  
41 114 the presence of significant vertical velocities.

42  
43  
44 115 The present work represents the first development of an analogous FSLE  
45 116 technique applied to HF radar currents in the Adriatic Sea. This study aims at

1  
2  
3  
4  
5  
6  
7  
8  
9  
10  
11  
12  
13  
14  
15  
16  
17  
18  
19  
20  
21  
22  
23  
24  
25  
26  
27  
28  
29  
30  
31  
32  
33  
34  
35  
36  
37  
38  
39  
40  
41  
42  
43  
44  
45  
46  
47  
48  
49  
50  
51  
52  
53  
54  
55  
56  
57  
58  
59  
60  
61  
62  
63  
64  
65

117 determining transport patterns in the Northeastern Adriatic Sea during Bora  
118 and Sirocco events. This goal will be achieved by analyzing the high-resolution  
119 current measurements from the NASCUM radar network with the FSLE tech-  
120 nique. This work will also focus on several methodological aspects concerning  
121 the application of the FSLEs technique to radar datasets. This is particularly  
122 important since radar velocity fields are highly variable and cover smaller do-  
123 mains compared to satellite and numerical model fields used in previous studies.  
124 The sensitivity of the technique to different configurations of the FSLE param-  
125 eters will be discussed.

126 The paper is organized as follows: in Section 2 the datasets and the developed  
127 FSLE algorithm are described. Section 3 shows the results of the sensitivity  
128 analysis for different FSLE parameter settings and describes the LCSs maps  
129 obtained for different wind regimes. Finally, the discussion of results and the  
130 conclusions are presented in Section 4.

131 **2. Data and Methods**

132 *2.1. Wind episodes identification*

133 The FSLE analysis on sea surface currents is applied during periods charac-  
134 terized by strong, long-lasting events of Bora and Sirocco. In order to identify  
135 the most relevant wind episodes over the radar area, several datasets have been  
136 used, i.e. measured wind and sea level (SL) from different meteo-mareographic  
137 stations along the Northern Italian coast (Figure 1). The wind data in Tri-  
138 este, come from the meteo-oceanographic buoy, MAMBO-1, managed by OGS  
139 (*Istituto Nazionale di Oceanografia e di Geofisica Sperimentale*<sup>1</sup>). The wind  
140 time series in Venice are recorded at the Acqua Alta platform by ISMAR-CNR  
141 (*Istituto di Scienze Marine - Consiglio Nazionale delle Ricerche*<sup>2</sup>). While the  
142 SL time series are provided by ISPRA (*Istituto Superiore per la Ricerca e la*

---

<sup>1</sup><http://www.ogs.trieste.it/>

<sup>2</sup><http://www.ismar.cnr.it/>

1  
2  
3  
4  
5  
6  
7  
8  
9 143 *Protezione Ambientale*<sup>3</sup>).

10 144 The hourly wind data have been low-pass filtered (33 h LP) to remove  
11  
12 145 diurnal-period oscillations, associated with the sea-breeze regime [Cosoli et al.,  
13  
14 146 2012]. The same filter has been applied to the hourly SL series to remove tidal  
15  
16 147 harmonics and Adriatic seiches.

17 148 Bora events have been detected from the filtered wind time-series of the  
18  
19 149 Trieste station (Figure 2, upper panels). The episodes of Bora are defined when  
20  
21 150 at least 75% of the wind vectors, over a window of 3 days minimum, blow from  
22  
23 151 the first quadrant [i.e. between North and East, Ursella et al., 2006], with speed  
24  
25 152 greater than 5m/s.

26 153 The Sirocco events have been identified from the filtered wind data of the  
27  
28 154 Venice station (Figure 2, central panels). The episodes of strong Sirocco are  
29  
30 155 defined when at least 75% of the wind vectors, over a window of 3 days minimum,  
31  
32 156 blow from S-SE, with speed at least equal to 5m/s. Moreover, the effects of the  
33  
34 157 Sirocco occurrence have been identified from the tide-gauge measurements in  
35  
36 158 Venice station (Figure 2, bottom panel). In fact, the Sirocco piles up sea water  
37  
38 159 along the northernmost border of the Adriatic Sea, leading to the SL rise along  
39  
40 160 the northern Adriatic coast [Orlić et al., 1994]. A further contribution to the  
41  
42 161 SL rise may be also given by the large low atmospheric pressure structure with  
43  
44 162 weak horizontal pressure gradients, which however drives Sirocco itself [Poulain  
45  
46 163 and Raicich, 2001].

47 164 Calm wind periods have also been investigated as a term of comparison.  
48  
49 165 These are defined as periods of at least seven days with wind intensity lower  
50  
51 166 than 3 m/s.

52 167 The wind episodes are selected in the period limited to the widest available  
53  
54 168 radar coverage (February 2008 - August 2008, see Cosoli et al. [2012]). Such  
55  
56 169 conditions allow for better performances of the FSLE method, since particles  
57  
58 170 can be advected in a wider domain.

59 171 For each wind regime the most significant events have been selected in order

---

56 <sup>3</sup><http://www.mareografico.it/>

1  
2  
3  
4  
5  
6  
7  
8  
9 172 to evidence possible recurrent features in the detected LCSs. The identified  
10 173 wind events are summarized as follows (see Figure 2): the episodes of Bora of  
11 174 the 4-8 March 2008 and of Sirocco of the 14-18 May 2008, are the strongest  
12 175 wind manifestations for the entire period considered. *These wind episodes were*  
13 176 *also identified* by Mihanović et al. [2011] for describing the sea surface current  
14 177 patterns during typical wind episodes. An additional episode of weak Bora (12-  
15 178 15 June 2008) is shown for comparison with the strong Bora case. The longest  
16 179 calm wind period is found between 17-29 February 2008.

17 180 The different temporal length of these episodes does not affect the analysis  
18 181 since the particles, launched for the evaluation of the FSLE, are initialized in the  
19 182 period of interest, but their evolution is not forced to stop at the limits of this  
20 183 period. However, they can leave the velocity field according to the transport  
21 184 properties of the currents themselves.

22 185 The occurrence of these wind episodes has been further confirmed by high-  
23 186 resolution modeled wind fields coming from ALADIN/HR (*Aire Limitée Adap-*  
24 187 *tation dynamique Développement InterNational*), run by the Croatian Meteorolo-  
25 188 gical and Hydrological Service<sup>4</sup>. ALADIN/HR wind maps are available with  
26 189 2 km spatial resolution and 3 hours temporal resolution (not shown).

## 27 190 2.2. HF surface currents

28 191 The installed NASCUM network was composed of 3 CODAR (Coastal Ocean  
29 192 Dynamics Application Radar) Sea Sonde HF radar stations (dots in Figure 1),  
30 193 active from August 2007 to August 2008. Two stations were located along the  
31 194 Istrian coast (in Rt Zub and Savudrija) and the third one, included since De-  
32 195 cember 2007, on the Italian coast (in Bibione - Punta Tagliamento). The radars  
33 196 were set up in the 25 MHz frequency at 100 kHz bandwidth, allowing a range  
34 197 up to 50 km offshore with 1.5 km radial resolution and 5° angular resolution.  
35 198 Surface currents are mapped over a regular grid of about 30 km × 20 km (max-  
36 199 imum coverage) with 2 km spatial resolution and 1 h temporal resolution. The

---

37  
38  
39  
40  
41  
42  
43  
44  
45  
46  
47  
48  
49  
50  
51  
52  
53  
54  
55  
56 <sup>4</sup>[http://meteo.hr/index\\_en.php/](http://meteo.hr/index_en.php/)



1  
2  
3  
4  
5  
6  
7  
8  
9  
200 current field covers the eastern and shallowest part of the Northern Adriatic  
201 with bottom depth from 20 m to 40 m, right in between the northern Bora  
202 “corridors” and directly affected by the Tagliamento river output (Figure 1).

203 The HF current dataset <sup>5</sup> comes from the processing of the raw radial mea-  
204 surements performed by Cosoli et al. [2012]. For more information about the  
205 treatment, the reader is referred to Chapman and Graber [1997] and Kovačević  
206 et al. [2004]. The current signal includes also the tidal component. Episodi-  
207 cally, current fields show some missing values at few points of the grid close to  
208 the baseline Bibione-Savudrija. This is due to the constraints in the intersect-  
209 ing beam geometry, required to minimize the effects of the site-to-site baseline  
210 instabilities. Therefore, a linear interpolation has been applied in order to com-  
211 plete the gap in the grid nodes to avoid the problem of truncated trajectories  
212 due to missing velocity values.

### 213 *2.3. FSLE application*

214 The FSLEs are evaluated by measuring the time needed for a particle pair  
215 to separate from an initial distance  $\delta_i$  to a final distance  $\delta_f$ . Thus, the analy-  
216 sis developed for this study includes two stages: first, the computation of the  
217 synthetic trajectories; second, the code which evaluates the FSLE and maps  
218 the final result. Particles trajectories are calculated by discretizing the advec-  
219 tion equation and applying the 4<sup>th</sup> order explicit Runge-Kutta method with a 4  
220 point bilinear interpolation [Hernández-Carrasco et al., 2011]. The values of  $\delta_i$   
221 and  $\delta_f$  influence the identification of the LCSs in the flow field, and depend on  
222 the characteristics of the flow field itself, on the length scale of the structures of  
223 interest and on the size of the domain. The initial distance affects the visibility  
224 of the details (the smaller  $\delta_i$ , the more details), as the resolution of the grid  
225 where the FLSEs are computed is chosen to be equal to the initial distance  
226 between particles [d’Ovidio et al., 2004; Lehahn et al., 2007]. This ensures that  
227 all the space in the velocity field is sampled once and just once. On the other

---

<sup>5</sup>[http://poseidon.ogs.trieste.it/jungo/NASCUM/index\\_en.html](http://poseidon.ogs.trieste.it/jungo/NASCUM/index_en.html)

1  
2  
3  
4  
5  
6  
7  
8  
9  
10  
11  
12  
13  
14  
15  
16  
17  
18  
19  
20  
21  
22  
23  
24  
25  
26  
27  
28  
29  
30  
31  
32  
33  
34  
35  
36  
37  
38  
39  
40  
41  
42  
43  
44  
45  
46  
47  
48  
49  
50  
51  
52  
53  
54  
55  
56  
57  
58  
59  
60  
61  
62  
63  
64  
65

228 hand, the final distance influences the detection of the structures (with larger  
229  $\delta_f$ , only the most stable and intense structures emerge).

230 Once these parameters are chosen, the FSLE are computed by launching an  
231 ensemble of synthetic particles over the FSLE grid and following the evolution of  
232 their relative distance. For each node of the FSLE grid, five particles are initial-  
233 ized with a central particle located over the grid node and the other four placed  
234 around it at a distance  $\delta_i$  along the latitudinal and longitudinal directions. This  
235 choice allows to account for the different intensity of dispersion along different  
236 directions [Boffetta et al., 2001] in order to retain the fastest diverging couples.  
237 FSLEs are computed every 3 hours using both forward and backward integra-  
238 tion in time, which allow to identify both the strongest repulsive and attractive  
239 LCSs during different wind regimes. Values of the FSLE  $\lambda$  are calculated at  
240 each node according to the definition [Sandulescu et al., 2007]:

241 • forward integration:

$$\lambda^+ = \frac{1}{\tau} \ln \frac{\delta_f}{\delta_i};$$

242 • backward integration:

$$\lambda^- = -\frac{1}{\tau} \ln \frac{\delta_f}{\delta_i};$$

243 where  $\tau$  is the time needed to separate two particles of the ensemble from  $\delta_i$   
244 up to  $\delta_f$ . The faster the divergence, the smaller is  $\tau$ , and the larger (in absolute  
245 value) is  $\lambda$ . It is important to remark, that divergence in backward integration  
246 actually identifies regions of convergence of the flow. If one of the particles of  
247 an ensemble leaves the velocity field before  $\delta_f$  is reached, then  $\lambda$  is **not** defined.  
248 Maximum values of the  $\lambda^+$  and  $\lambda^-$  fields identify repulsive and attractive LCSs,  
249 respectively. The maps in this paper present tangles of attractive and repulsive  
250 LCSs obtained by superposing both forward and backward integration FSLE  
251 fields [Molcard et al., 2006].

1  
2  
3  
4  
5  
6  
7  
8  
9 **3. Results**

10  
11 *3.1. FSLE method set up*

12  
13 The application of the FSLE algorithm to the radar current field requires  
14 to set up the parameters defining initial and final separation distance between  
15 particles,  $\delta_i$  and  $\delta_f$  respectively. Since there are no previous studies on FSLE  
16 analysis in the Northeastern Adriatic Sea, an overview on the sensitivity analysis  
17 performed on the  $\delta_i$  and  $\delta_f$  parameters for this particular case study is presented.  
18  
19

20  
21 In general, a suitable combination of the two parameters must be chosen. This  
22 should take into account that although  $\delta_i$  can be fixed arbitrarily small, there  
23 is an intrinsic limit on the details of the resulting structures which is associated  
24 with the surface shear information captured in the current field itself. Fur-  
25 thermore, if  $\delta_f$  is chosen larger than the separation distance achievable by the  
26 particles advected within the finite spatial domain of HF radar velocities, no  
27 structures will be detected from the flow field.  
28  
29

30  
31 Given the characteristics of the dataset and the focus of the present work,  
32 we aim at identifying the transport structures associated with small-scale (i.e.  
33 mesoscale) processes. The horizontal scale of mesoscale processes is represented  
34 by the internal Rossby radius of deformation, which is about 3-5 km in the  
35 Middle and Northern Adriatic [Masina and Pinardi, 1994]. However, eddies can  
36 have even smaller size during winter when waters are completely mixed and  
37 the first baroclinic Rossby radius of deformation almost vanishes [Bergamasco  
38 et al., 1996]. Recent numerical findings from a climatic circulation model of  
39 the northern Adriatic Sea confirm values around 3km in spring [Malačić et al.,  
40 2012].  
41  
42

43  
44 In order to find a choice of parameters able to identify appropriately both  
45 weak and strong LCSs during any of the wind regimes considered, several tests  
46 for all the wind cases have been performed (not shown). The following results  
47 are representative of calm wind, but are purposefully shown in order to evidence  
48 how the characteristics of the FSLE field, and thus of the identified LCSs, change  
49 depending on the chosen parameter values.  
50  
51  
52  
53  
54  
55  
56  
57  
58  
59  
60  
61  
62  
63  
64  
65

1  
2  
3  
4  
5  
6  
7  
8  
9  
10  
11  
12  
13  
14  
15  
16  
17  
18  
19  
20  
21  
22  
23  
24  
25  
26  
27  
28  
29  
30  
31  
32  
33  
34  
35  
36  
37  
38  
39  
40  
41  
42  
43  
44  
45  
46  
47  
48  
49  
50  
51  
52  
53  
54  
55  
56  
57  
58  
59  
60  
61  
62  
63  
64  
65

282 As a first trial, according to the value of the Rossby radius,  $\delta_f$  is fixed to 3  
283 km and several FSLE maps obtained for different  $\delta_i$  are compared (Figure 3).  
284 Starting from an initial distance between particles equal to the resolution of  
285 the radar velocity field (2 km) and successively reducing the parameter  $\delta_i$ , the  
286 detected LCSs keep their configuration while their features become sharper.  
287 This property of FSLE-based LCSs has been first recognized by Hernández-  
288 Carrasco et al. [2011], who identified it as fractal behavior. At the same time,  
289 it is important to remark that by reducing  $\delta_i$  the number of particles used in  
290 the analysis, and thus its computational requirements, increases. Considering  
291 the radar field resolution and the scales of interest,  $\delta_i=0.4$  km represents a good  
292 compromise between the FSLE map resolution and the computational efficiency  
293 to resolve structures within the range of few kilometers. Once the value of  $\delta_i$   
294 is set, an analysis on the sensitivity of the detected LCSs for different values  
295 of  $\delta_f$  is also performed. Since mesoscale ranges within less than 3 km up to  
296 about 5 km, different values of  $\delta_f$  were tested from 1 km to 5 km (Figure 4).  
297 Usually just a limited group of particle couples is able to reach the relative  
298 final distance chosen, depending on the spatial extension of the current field  
299 and on the surface shear caught by radar measurement. Moreover the greater  
300 the final distance is, the longer will be the time required for each couple to  
301 separate up to this value. Therefore for small  $\delta_f$  a lot of couples separate in  
302 very short time and the structures in the FSLE map are very broad and almost  
303 indistinguishable from one another, since they are detected also for very weak  
304 transport structures. On the other hand for large  $\delta_f$  fewer particles separate  
305 up to this value and the resulting structures are formed by only few points of  
306 the map. These are associated with the stronger, more persistent structures,  
307 which therefore are more relevant for characterizing the transport properties of  
308 the flow. This is true especially in strong wind cases (not shown) when currents  
309 are so strong and coherent in space that for  $\delta_f=3$  km all the particles leave the  
310 radar field before having reached the fixed final distance, so that the transport  
311 structures cannot be identified at all. In conclusion, the final distance which  
312 allows the identification of transport structures for any wind condition under

1  
2  
3  
4  
5  
6  
7  
8  
9 study is  $\delta_f=1.6$  km.

### 10 11 12 3.2. LCS patterns during wind episodes

13  
14 To investigate the changes in the LCS patterns with different wind condi-  
15 tions, several episodes for each wind regime have been analyzed and the most  
16 representative cases are presented in Figures 5 to 7. These maps show the  
17 FSLE field for a time centered within a given wind episode, to ensure that the  
18 dynamical conditions just before and after this period do not affect the tra-  
19 jectories evolution at the sea surface. In the figures, repulsive LCSs (FSLE  
20 maxima/separating trajectories) are in red, whereas attractive LCSs (FSLE  
21 minima/converging trajectories) are in blue.  
22  
23

24  
25 For the calm wind case in February the spatial configuration of the trans-  
26 port structures is quite broad and detailed (Figure 5). Several attractive and  
27 repulsive LCSs are identified and they cross each other within the radar ve-  
28 locity field. These transport structures evolve with a longer time scale (up to  
29 3-4 days), independently from the high temporal variability characterizing the  
30 velocity field (due to tidal oscillations in the diurnal and semidiurnal frequency  
31 bands and near-inertial oscillations, as observed by Cosoli et al. [2012]). This is  
32 a typical feature of LCSs since they result from the integration of trajectories  
33 over time scales much longer than the ones characterizing the variability of the  
34 velocity field.  
35  
36

37  
38 An attractive LCS is present in front of the Italian coast throughout the  
39 entire calm wind period. The structure marks the convergence between GoT  
40 and Northern Adriatic waters. Its eastern half is oriented South-East to North-  
41 West, as mean advection goes from the Istrian coast toward the river mouth  
42 of the Tagliamento. There, it forms a right angle with the Italian coastline  
43 direction, because the jet along the Italian coast is deviated by the fresh water  
44 output from the Tagliamento river. Cosoli et al. [2012] observed an analogous  
45 deviation of the surface currents in front of the Tagliamento estuary.  
46  
47

48  
49 A repulsive structure occupies the central part of the current field and crosses  
50 the attractive structure facing the entrance of the GoT and other weaker at-  
51  
52  
53  
54  
55  
56  
57  
58

1  
2  
3  
4  
5  
6  
7  
8  
9  
10  
11  
12  
13  
14  
15  
16  
17  
18  
19  
20  
21  
22  
23  
24  
25  
26  
27  
28  
29  
30  
31  
32  
33  
34  
35  
36  
37  
38  
39  
40  
41  
42  
43  
44  
45  
46  
47  
48  
49  
50  
51  
52  
53  
54  
55  
56  
57  
58  
59  
60  
61  
62  
63  
64  
65

343 tractive structures in the field. The attractive structure to the south-east of the  
344 radar field is associated to an anticyclonic vortex in front of the Istrian coast.  
345 The current field presents several patterns with length scale larger than the  
346 internal Rossby radius of deformation identified by Masina and Pinardi [1994].  
347 The mesoscale length and variability also depends on stratification conditions  
348 and can be several times smaller/bigger than the internal radius of deformation  
349 (about 5km), as observed also by Bergamasco et al. [1996]. For this reason, in  
350 order to compare this case to the other wind episodes, the analysis will focus on  
351 the pattern that can be considered recurrent, that is the strongest attractive fil-  
352 ament at the entrance of GoT, related to the water exchange between the North  
353 Adriatic and the gulf itself (process already observed in the seasonal mesoscale  
354 study by Malačić and Petelin [2009]).

355 The FSLE analysis in the Bora case focuses on the March episode (Fig-  
356 ure 6(a)). Before and after the Bora event, wind conditions are predominantly  
357 calm and the spatial organization of LCSs is similar to the calm case of February  
358 just described. The response of the surface current to Bora wind is almost in-  
359 stantaneous, showing the development of intense westward/south-westward cur-  
360 rents throughout the radar domain. This is in agreement with the observations  
361 from Cosoli et al. [2012]; Malačić et al. [2012]; Mihanović et al. [2011]. Along  
362 the Istrian coastline, these currents are weaker than the ones further north. The  
363 resulting meridional current shear reflects the wind pattern over this part of the  
364 Adriatic basin: Bora is stronger along the northern “corridor”, and weaker to  
365 the south where it is screened by coastal orography. This north-south current  
366 shear introduces cyclonic vorticity extending far off from the Istrian coast, as  
367 already observed by Cosoli et al. [2012].

368 The evolution of the LCSs during Bora cases is characterized by a sequence of  
369 recurrent patterns: at the beginning of the Bora episode the attractive LCS typ-  
370 ical of calm wind conditions (Figure 5) is still present in the northernmost part  
371 of the radar domain in front of the Italian coastline. The structure remains sta-  
372 ble until the Bora has fully developed (not shown), but it is not present anymore  
373 as soon as the westward current pattern extends over the whole Northeastern

1  
2  
3  
4  
5  
6  
7  
8  
9  
10  
11  
12  
13  
14  
15  
16  
17  
18  
19  
20  
21  
22  
23  
24  
25  
26  
27  
28  
29  
30  
31  
32  
33  
34  
35  
36  
37  
38  
39  
40  
41  
42  
43  
44  
45  
46  
47  
48  
49  
50  
51  
52  
53  
54  
55  
56  
57  
58  
59  
60  
61  
62  
63  
64  
65

374 Adriatic (Figure 6(a)).

375       The disappearance of this attractive transport structure during Bora episodes,  
376 and its reappearance as soon as Bora ceases, indicates that the LCS does not  
377 vanishes but it is just displaced westward outside the radar domain by the pres-  
378 ence of the intense, homogeneous Bora-driven currents. This can be evidenced  
379 through the analysis of an episode of weak Bora, such as the one identified in  
380 June 2008 (Figure 6(b)). The initial evolution of the transport structures is  
381 analogous to the strongest Bora case already analyzed. In fact, at the begin-  
382 ning of the Bora episode an attractive LCS is present to the north of the radar  
383 domain. However, during such event, the Bora-driven westward currents are less  
384 homogeneous over the basin, so that the region of convergence is still present in  
385 front of the Italian coast.

386       The development of a repulsive LCS in front of the Istrian coast is another  
387 common feature of both strong and weak Bora episodes. However, during the  
388 weaker events, this LCS is less intense **but more extended** than the one devel-  
389 oping during the strong ones.

390       The FSLE analysis in case of Sirocco forcing focuses on the event in May 2008  
391 (Figure 7). Regardless of the currents configuration before a Sirocco event, as  
392 soon as Sirocco starts to blow it induces an homogeneous north-northeastward  
393 current. After the Sirocco has reached a steady state, this uniform current,  
394 developed throughout all the radar field, induces the piling up of surface waters  
395 in the northern part of the basin. **A part of this water mass converges along the**  
396 **attractive LCS, stretched from SW to NE, and enters the GoT mostly along the**  
397 **northern (Italian) coastline. The intensified inflow along the northern side of the**  
398 **GoT is also supported by recent numerical model findings [Malačić et al., 2012].**  
399 The transport associated with this LCS is from West to East, which is reversed  
400 with respect to the calm wind case when waters flow cyclonically following the  
401 basin coastline. On the other hand, the meridional part of the flow field does not  
402 show intense structures, since the currents are rather uniform in direction and  
403 intensity and the advected particles do not experience the shear necessary to  
404 diverge or converge. When Sirocco relaxes the cyclonic gyre is gradually restored

1  
2  
3  
4  
5  
6  
7  
8  
9  
10  
11  
12  
13  
14  
15  
16  
17  
18  
19  
20  
21  
22  
23  
24  
25  
26  
27  
28  
29  
30  
31  
32  
33  
34  
35  
36  
37  
38  
39  
40  
41  
42  
43  
44  
45  
46  
47  
48  
49  
50  
51  
52  
53  
54  
55  
56  
57  
58  
59  
60  
61  
62  
63  
64  
65

405 so that the eastward current along Italy returns and the transport associated  
406 to the attractive LCS reverses back in westward direction (not shown).

407 **4. Discussion and conclusions**

408 The surface transport in the Northeastern Adriatic Sea has been investi-  
409 gated by applying the FSLE technique on the current field detected by the HF  
410 coastal radar network active in the period from August 2007 to August 2008.  
411 The analysis is limited to the period from February 2008 to August 2008, when  
412 the spatial coverage of radar measurements was maximized under the three-site  
413 configuration. The interest is focused on the surface dynamics of this area asso-  
414 ciated with the typical wind regimes, Bora and Sirocco, compared to calm wind.  
415 Previous studies [d’Ovidio et al., 2009; García-Olivares et al., 2007] have con-  
416 firmed the advantage of using the FSLE technique over more traditional Eulerian  
417 diagnostics for detecting the transport structures which separate dynamically  
418 distinct regions of a flow. Moreover, compared to other Lagrangian diagnostics,  
419 such as the analysis of sparse drifter trajectories, the FSLE technique allows to  
420 retrieve information over broader domains, and thus is better suited for studies  
421 at the regional scale. Being the very first time that FSLE technique is applied  
422 to HF radar current fields of the Northern Adriatic Sea, it has been of crucial  
423 importance to investigate the sensitivity of the FSLE analysis with respect to  
424 the key parameters (initial distance,  $\delta_i$ , and final separation distance of parti-  
425 cles,  $\delta_f$ ) that control structures coverage and details visibility. Despite the very  
426 high variability of the radar current fields, the **reasonably chosen values** of these  
427 parameters has allowed to identify and investigate the evolution of the strongest  
428 transport structures.

429 In summary, the FSLE analysis on the current field revealed the presence of  
430 recurrent surface transport structures during the different wind regimes consid-  
431 ered (calm period, Bora and Sirocco). The current field during the calm wind  
432 period is characterized by the presence of multiple structures. Their persistence  
433 in time is longer when compared to the other wind cases analyzed. An attractive



1  
2  
3  
4  
5  
6  
7  
8  
9  
10  
11  
12  
13  
14  
15  
16  
17  
18  
19  
20  
21  
22  
23  
24  
25  
26  
27  
28  
29  
30  
31  
32  
33  
34  
35  
36  
37  
38  
39  
40  
41  
42  
43  
44  
45  
46  
47  
48  
49  
50  
51  
52  
53  
54  
55  
56  
57  
58  
59  
60  
61  
62  
63  
64  
65

434 LCS crosses the GoT entrance where the gulf and the North Adriatic waters  
435 converge. A repulsive structure is present in the central part of the radar field.  
436 The transport structures identified in strong Bora episodes show the displace-  
437 ment of the attractive LCS from the GoT entrance further west. Moreover a  
438 repulsive structure develops in front of the Istrian coast. On the other hand,  
439 during Sirocco events an attractive structure is present along the Italian coast.  
440 The transport associated with this LCS is from west to east, opposite to the  
441 calm wind case. This LCS indicates that Adriatic waters pile up along the  
442 northern coast.

443 As already pointed out, the surface circulation of the GoT is characterized  
444 by an outflowing transversal current developing from its southern border to the  
445 Tagliamento estuary, that merges with the westward flow along the Italian coast  
446 [Malačić and Petelin, 2009]. This FSLE analysis identifies an attractive LCS  
447 in front of the GoT entrance, which is associated with the transport driven  
448 by this transversal current out of the GoT. This structure is present in all the  
449 considered wind regimes but its location with respect to the Italian coast and  
450 the direction of transport associated with it varies.

451 During calm wind periods the attractive LCS extends from the northern  
452 Istrian tip to the Tagliamento river and further west, representing the barrier  
453 to the outflow of GoT waters to the Northern Adriatic Sea. The advection  
454 associated with this LCS is westward, in agreement with the diagonal current  
455 pattern typical of the GoT: surface waters entering the gulf along the Istrian  
456 coast and exiting from the Italian side of the GoT in a cyclonic pattern [Malačić  
457 and Petelin, 2001].

458 During weak Bora events, the attractive LCS is displaced westward with  
459 respect to its position in calm wind periods. The spatial configuration of this  
460 LCS with respect to the gulf entrance shows the location where the GoT surface  
461 waters extends to meet the Northern Adriatic coastal flow. On the other hand  
462 during strong Bora events there is no more evidence of the attractive LCS in  
463 the radar field, indicating that the convergence area, and thus the boundary of  
464 westward outflow from the GoT, could be positioned beyond the western limit

1  
2  
3  
4  
5  
6  
7  
8  
9  
10  
11  
12  
13  
14  
15  
16  
17  
18  
19  
20  
21  
22  
23  
24  
25  
26  
27  
28  
29  
30  
31  
32  
33  
34  
35  
36  
37  
38  
39  
40  
41  
42  
43  
44  
45  
46  
47  
48  
49  
50  
51  
52  
53  
54  
55  
56  
57  
58  
59  
60  
61  
62  
63  
64  
65

465 of the radar domain. A spatially coherent outflow from the GoT can indeed  
466 be observed from the radar measurements. This is in agreement with Malačić  
467 and Petelin [2009], who observed a similar outflow in response of intense wind  
468 forcing, and with Mihanović et al. [2011] who observed that Bora drives a sea  
469 level decrease in Trieste and, at the same time, a sea level rise in Venice.

470 To accurately identify the outflow barrier during strong Bora episodes, a  
471 wider current field would be necessary, either by extending westward the radar  
472 network or by using modeled current fields. In either weak and strong Bora cases  
473 a repulsive LCS develops in front of the Istrian coast. This structure represents  
474 a real transport barrier for the water masses present to the north and south of  
475 it. Any surface tracer present to the south of this repulsive LCS will not cross  
476 it and, therefore, the northward flow along the coast, characteristic of calm  
477 wind conditions, is temporarily halted. This determines a reduced connectivity  
478 between the Istrian coast and the GoT. This LCS could represent the southern  
479 boundary of the northern jet current exiting from the GoT and developing as a  
480 consequence of the Bora funneling between Dinaric Alps.

481 During Sirocco episodes the position of the attractive structure is found  
482 northeastward, as a consequence of the piling up of waters along the northern  
483 Adriatic coasts. Therefore there is no transport barrier in front of the GoT,  
484 indicating the occurrence of an extended inflow of North Adriatic waters into  
485 the GoT. Such inflow in the gulf is also confirmed by the observed sea level rise  
486 in Trieste during analogous wind events [Mihanović et al., 2011]. In this case,  
487 the local transport along this LCS is from west to east, and not in the opposite  
488 direction as during the typical cyclonic circulation of the North Adriatic area.  
489 The SW-NE orientation of the attractive LCS might indicate that the inflow  
490 comes from the open Adriatic rather than from coastal regions.

491 The application of the FSLE method on HF radar currents in the Northeast-  
492 ern Adriatic area can provide important information about horizontal transport  
493 dynamics. Such information could be greatly improved with the further devel-  
494 opment of a network of observation in the Northern Adriatic, which could lead  
495 to more refined transport analysis.

1  
2  
3  
4  
5  
6  
7  
8  
9  
10  
11  
12  
13  
14  
15  
16  
17  
18  
19  
20  
21  
22  
23  
24  
25  
26  
27  
28  
29  
30  
31  
32  
33  
34  
35  
36  
37  
38  
39  
40  
41  
42  
43  
44  
45  
46  
47  
48  
49  
50  
51  
52  
53  
54  
55  
56  
57  
58  
59  
60  
61  
62  
63  
64  
65

496       Concerning potential applications of the FSLE method, it could be directly  
497 used in case of sea accidents or pollutant discharge to identify the possible path-  
498 ways of dispersion from reliable near-real time velocity fields. This will allow  
499 to identify the potential source area of the pollutant, and will provide a crucial  
500 information to circumscribe the intervention area and guide the emergency op-  
501 erations.

502

### *Acknowledgements*

The authors thank OGS, ISMAR-CNR and ISPRA for providing wind and sea level time series. The authors are grateful to Dr. Miroslav Gačić for supporting this work and for the stimulating discussion about the interpretation of the results. Gratitude is due to Dr. Annalisa Griffa for the precious suggestions during the development of the FSLE algorithm. Maristella Berta thanks MIO for the hospitality and financial support during her stay in Marseille for the advancement of scientific research. Maristella Berta shows her appreciation to Dr. Angelique Haza for sharing with the authors her experienced opinion about the results of this work.

### **References**

### **References**

Artegiani, A., Bregant, D., Paschini, E., Pinardi, N., Raicich, F., Russo, A.,  
1997a. The Adriatic Sea general circulation. Part II: baroclinic circulation  
structure. *J. Phys. Oceanogr.* 27, 1515–1532.

Artegiani, A., Bregant, D., Paschini, E., Pinardi, N., Raicich, F., Russo, A.,  
1997b. The Adriatic Sea general circulation. Part I: air-sea interactions and  
water masses structure. *J. Phys. Oceanogr.* 27, 1492–1514.

- 1  
2  
3  
4  
5  
6  
7  
8  
9 Bergamasco, A., Gačić, M., Boscolo, R., Umgiesser, G., 1996. Winter oceanographic conditions and water masses balance in the Northern Adriatic (February 1993). *J. Marine Syst.* 7, 67–94.
- 10  
11  
12  
13  
14 Boffetta, G., Lacorata, G., Redaelli, G., Vulpiani, A., 2001. Detecting barriers  
15 to transport: a review of different techniques. *Physica D* 159, 58–70.
- 16  
17  
18 Bogunović, B., Malačić, V., 2009. Circulation in the Gulf of Trieste:  
19 measurements and model results. *Il Nuovo Cimento (C)* 31, 301–326.  
20 Doi:10.1393/ncc/i2008-10310-9.
- 21  
22  
23 Chapman, R., Graber, H., 1997. Validation of (HF) radar measurements.  
24 *Oceanography* 10, 76–79.
- 25  
26  
27 Cosoli, S., Gačić, M., Mazzoldi, A., 2012. Surface current variability and wind  
28 influence in the Northern Adriatic Sea as observed from High-Frequency (HF)  
29 radar measurements. *Cont. Shelf Res.* 33, 1–13.
- 30  
31  
32  
33 d’Ovidio, F., Fernández, V., Hernández-García, E., López, C., 2004. Mixing  
34 structures in the Mediterranean Sea from Finite-Size Lyapunov Exponents.  
35 *Geophys. Res. Lett.* 31.
- 36  
37  
38 d’Ovidio, F., Isern-Fontanet, J., López, C., Hernández-García, E., García-  
39 Ladona, E., 2009. Comparison between Eulerian diagnostics and finite-size  
40 Lyapunov exponents computed from altimetry in the Algerian basin. *Deep-  
41 Sea Res. I* 56, 15–31.
- 42  
43  
44  
45 Ferrarese, S., Cassardo, C., Elmi, A., Genovese, R., Longhetto, A., Manfrin, M.,  
46 Richiardone, R., 2008. Response of temperature and sea surface circulation  
47 to a Sirocco wind event in the Adriatic basin: a model simulation. *J. Marine  
48 Syst.* 74, 659–671.
- 49  
50  
51  
52 García-Olivares, A., Isern-Fontanet, J., García-Ladona, E., 2007. Dispersion of  
53 passive tracers and finite-scale Lyapunov exponents in the Western Mediter-  
54 ranean Sea. *Deep-Sea Res. I* 54, 253–268.
- 55  
56  
57  
58

- 1  
2  
3  
4  
5  
6  
7  
8  
9 Gurgel, K.W., Antonischski, G., Essen, H.H., Schlick, T., 1999. Wellen radar  
10 (WERA): a new ground-wave hf radar for ocean remote sensing. *Coast. Eng.*  
11 37, 219–234.  
12  
13  
14 Haza, A.C., Griffa, A., Martin, P., Molcard, A., Ozgokmen, T.M., Poje, A.C.,  
15 Barbanti, R., Book, J.W., Poulain, P.M., Rixen, M., Zanasca, P., 2007.  
16 Model-based directed drifter launches in the Adriatic Sea: results from the  
17 DART experiment. *Geophys. Res. Lett.* 34.  
18  
19  
20  
21 Haza, A.C., Ozgokmen, T.M., Griffa, A., Molcard, A., Poulain, P.M., Peggion,  
22 G., 2010. Transport dispersion processes in small-scale coastal flows: relative  
23 dispersion from VHF radar measurements in the Gulf of La Spezia. *Ocean*  
24 *Dynam.* 60, 861–882.  
25  
26  
27  
28 Haza, A.C., Poje, A.C., Ozgokmen, T.M., Martin, P., 2008. Relative dispersion  
29 from a high-resolution coastal model of the Adriatic Sea. *Ocean Model.* 22,  
30 48–65.  
31  
32  
33  
34 Hernández-Carrasco, I., López, C., Hernández-García, E., Turiel, A., 2011. How  
35 reliable are finite-size Lyapunov exponents for the assessment of ocean dy-  
36 nam.? *Ocean Model.* 36, 208–218.  
37  
38  
39 Jeffries, M.A., Lee, C.M., 2007. A climatology of the northern Adriatic Sea’s  
40 response to bora and river forcing. *J. Geophys. Res.* 112.  
41  
42  
43 Kovačević, V., Gačić, M., Mancero Mosquera, I., Mazzoldi, A., Marinetti, S.,  
44 2004. HF radar observation in the Northern Adriatic: surface current field in  
45 front of the Venetian Lagoon. *J. Marine Syst.* 51, 95–122.  
46  
47  
48 Kuzmić, M., Janeković, I., Book, J.W., Martin, P.J., Doyle, J.D., 2007. Model-  
49 ing the northern Adriatic double-gyre response to intense bora wind: a revisit.  
50 *J. Geophys. Res.* 112. Doi:10.1029/2005JC003377.  
51  
52  
53  
54 Lazar, M., Pavić, M., Pasarić, Z., Orlić, M., 2007. Analytical modelling of  
55 wintertime coastal jets in the Adriatic Sea. *Cont. Shelf Res.* 27, 275–285.  
56  
57  
58

- 1  
2  
3  
4  
5  
6  
7  
8  
9 Lazić, L., Tošić, I., 1998. A real data simulation of the Adriatic Bora and the  
10 impact of mountain height on the Bora trajectories. *Meteorol. Atmos. Phys.*  
11 66, 143–155.  
12  
13  
14 Lehahn, Y., d’Ovidio, F., Lévy, M., Heifetz, E., 2007. Stirring of the northeast  
15 Atlantic spring bloom: a Lagrangian analysis based on multisatellite data. *J.*  
16 *Geophys. Res.* 112.  
17  
18  
19 Malanotte-Rizzoli, P., Bergamasco, A., 1983. The dynamics of the coastal region  
20 of the Northern Adriatic Sea. *J. Phys. Oceanogr.* 13, 1105–1130.  
21  
22  
23 Malačić, V., Petelin, B., 2001. Regional studies. The gulf of Trieste., in:  
24 Cushman-Roisin, B., Gačić, M., Poulain, P.M., Artegiani, A. (Eds.), *Physical*  
25 *oceanography of the Adriatic Sea: past, present and future.* Kluwer Academic  
26 Publishers.  
27  
28  
29 Malačić, V., Petelin, B., 2009. Climatic circulation in the Gulf of Trieste (north-  
30 ern Adriatic). *J. Geophys. Res.* 114. Doi:10.1029/2008JC004904.  
31  
32  
33 Malačić, V., Petelin, B., Vodopivec, M., 2012. Topographic control of  
34 wind-driven circulation in the northern Adriatic. *J. Geophys. Res.* 117.  
35 Doi:10.1029/2012JC008063.  
36  
37  
38 Masina, S., Pinardi, N., 1994. Mesoscale data assimilation studies in the middle  
39 Adriatic Sea. *Cont. Shelf Res.* 14, 1293–1310.  
40  
41  
42  
43 Mihanović, H., Cosoli, S., Vilibić, I., Ivanković, D., Dadić, V., Gačić, M.,  
44 2011. Surface current patterns in the northern Adriatic extracted from high-  
45 frequency radar data using self-organizing map analysis. *J. Geophys. Res.*  
46 116. Doi:10.1029/2011JC007104.  
47  
48  
49  
50 Molcard, A., Poje, A.C., Ozgokmen, T.M., 2006. Directed drifter launch strate-  
51 gies for Lagrangian data assimilation using hyperbolic trajectories. *Ocean*  
52 *Model.* 12, 268–289.  
53  
54  
55  
56  
57  
58  
59  
60  
61  
62  
63  
64  
65

- 1  
2  
3  
4  
5  
6  
7  
8  
9 Nencioli, F., d'Ovidio, F., Doglioli, A.M., Petrenko, A.A., 2011. Surface coastal  
10 circulation patterns by in-situ detection of Lagrangian Coherent Structures.  
11 Geophys. Res. Lett. 38. Doi:10.1029/2011GL048815.  
12  
13  
14 Orlić, M., Gačić, M., La Violette, P.E., 1992. The currents and circulation of  
15 the Adriatic Sea. *Oceanol. Acta* 15, 109–124.  
16  
17  
18 Orlić, M., Kuzmić, M., Pasarić, Z., 1994. Response of the Adriatic Sea to the  
19 Bora and Sirocco forcing. *Cont. Shelf Res.* 14, 91–116.  
20  
21  
22 Ottino, J.M., 1989. *The kinematics of mixing: stretching, chaos and transport.*  
23 Cambridge University Press.  
24  
25  
26 Poulain, P.M., 2001. Adriatic Sea surface circulation as derived from drifter  
27 data between 1990 and 1999. *J. Marine Syst.* 29, 3–32.  
28  
29  
30 Poulain, P.M., Kourafalou, V.H., Cushman-Roisin, B., 2001. Northern Adriatic  
31 Sea, in: Cushman-Roisin, B., Gačić, M., Poulain, P.M., Artegiani, A. (Eds.),  
32 *Physical oceanography of the Adriatic Sea: past, present and future.* Kluwer  
33 Academic Publishers.  
34  
35  
36  
37 Poulain, P.M., Raicich, F., 2001. Forcings, in: Cushman-Roisin, B., Gačić, M.,  
38 Poulain, P.M., Artegiani, A. (Eds.), *Physical oceanography of the Adriatic*  
39 *Sea: past, present and future.* Kluwer Academic Publishers.  
40  
41  
42 Sandulescu, M., López, C., Hernández-García, E., Feudel, U., 2007. Plankton  
43 blooms in vortices: the role of biological and hydrodynamic timescales.  
44 *Nonlinear Proc. Geoph.* 14, 443–454.  
45  
46  
47  
48 Ursella, L., Poulain, P.M., Signell, R.P., 2006. Surface drifter derived circulation  
49 in the northern and middle Adriatic Sea: response to wind regime and season.  
50 *J. Geophys. Res.* 111. [printed 112(C3),2007].  
51  
52  
53 Yoshino, M.M., 1976. *Local wind Bora.* University of Tokyo Press.  
54  
55  
56 Zore, M., 1956. On gradient currents in the Adriatic Sea. *Acta Adriat.* 8, 1–38.  
57  
58  
59  
60  
61  
62  
63  
64  
65

1  
2  
3  
4  
5  
6  
7  
8  
9 Zore-Armanda, M., Gačić, M., 1987. Effect of Bura on the circulation in the  
10 Northern Adriatic. Ann. Geophys. 5B, 93-102.  
11  
12  
13  
14  
15  
16  
17  
18  
19  
20  
21  
22  
23  
24  
25  
26  
27  
28  
29  
30  
31  
32  
33  
34  
35  
36  
37  
38  
39  
40  
41  
42  
43  
44  
45  
46  
47  
48  
49  
50  
51  
52  
53  
54  
55  
56  
57  
58  
59  
60  
61  
62  
63  
64  
65



1  
2  
3  
4  
5  
6  
7  
8  
9  
10  
11  
12  
13  
14  
15  
16  
17  
18  
19  
20  
21  
22  
23  
24  
25  
26  
27  
28  
29  
30  
31  
32  
33  
34  
35  
36  
37  
38  
39  
40  
41  
42  
43  
44  
45  
46  
47  
48  
49  
50  
51  
52  
53  
54  
55  
56  
57  
58  
59  
60  
61  
62  
63  
64  
65

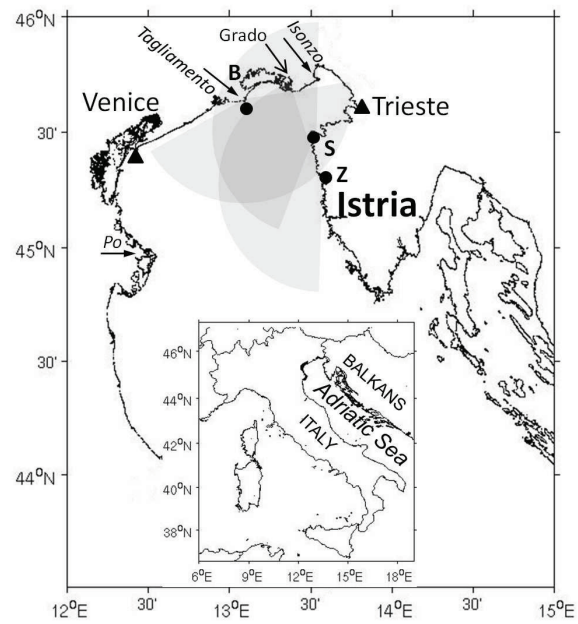


Figure 1: The data set coverage over the Northern Adriatic area with the radar stations (dots) in Bibione (B), Savudrija (S) and Rt Zub (Z). The meteo-mareographic stations in Trieste and Venice (triangles). The main river estuaries: Po, Tagliamento and Isonzo. The Gulf of Trieste is the sea area landlocked within Savudrija-Grado ideal baseline.

1  
2  
3  
4  
5  
6  
7  
8  
9  
10  
11  
12  
13  
14  
15  
16  
17  
18  
19  
20  
21  
22  
23  
24  
25  
26  
27  
28  
29  
30  
31  
32  
33  
34  
35  
36  
37  
38  
39  
40  
41  
42  
43  
44  
45  
46  
47  
48  
49  
50  
51  
52  
53  
54  
55  
56  
57  
58  
59  
60  
61  
62  
63  
64  
65

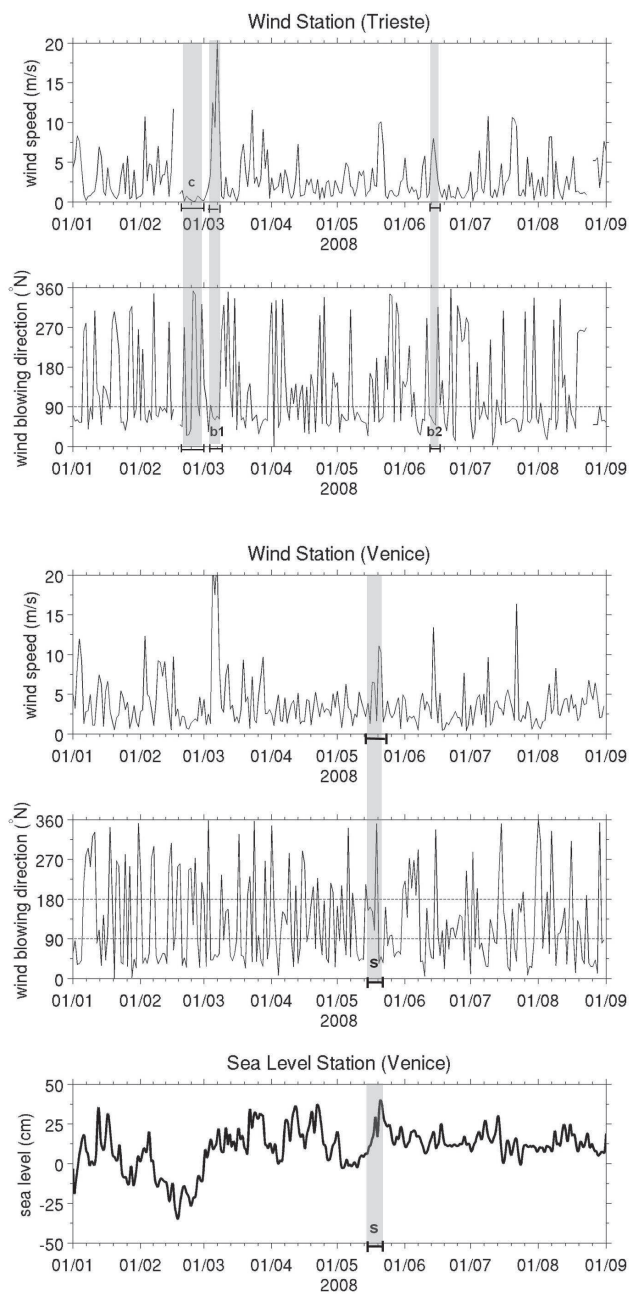


Figure 2: The wind periods selected: in the two upper panels the calm wind period (c) and the two Bora episodes (strongest b1 and weaker b2) from the wind time series in Trieste. The two panels in the middle indicate the Sirocco episode (s) identified from the wind time series in Venice. The lowest panel represents the sea level time series in Venice station with the selected Sirocco event (s).

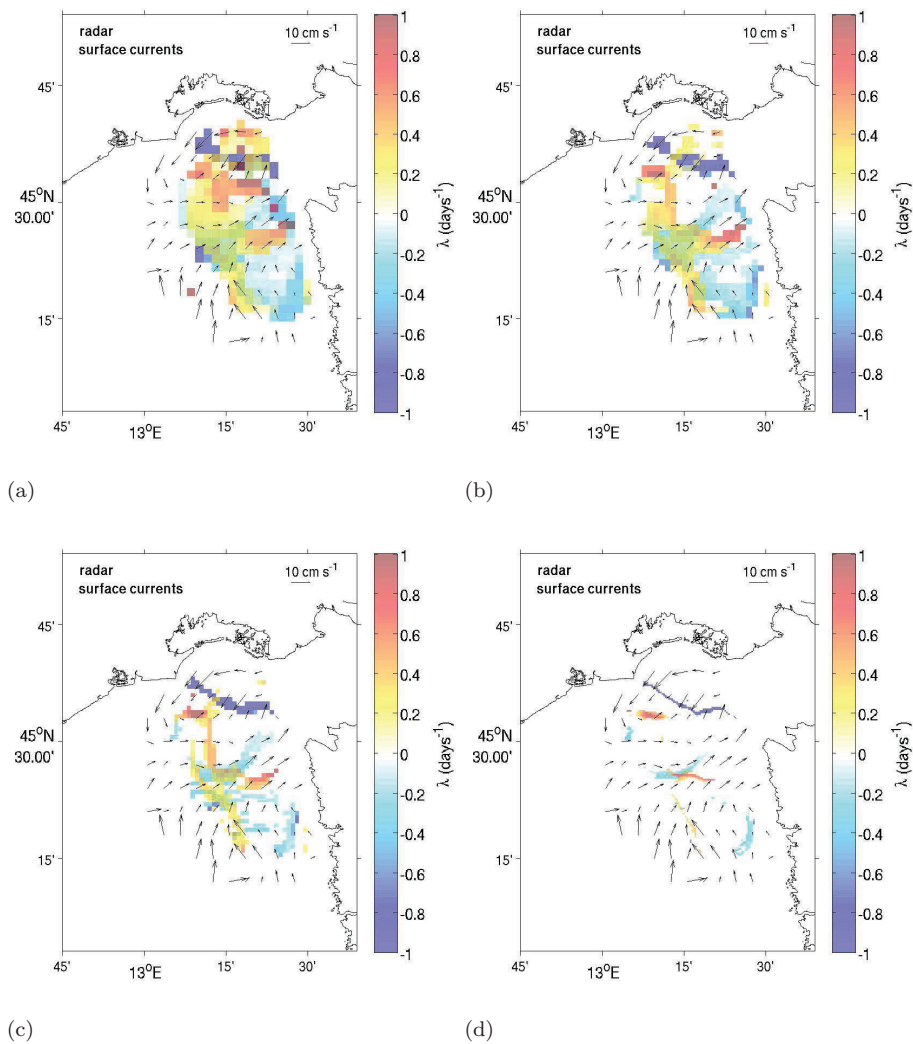


Figure 3: FSLE ( $\text{days}^{-1}$ ) trial maps for different  $\delta_i$ : (a) 2 km, (b) 1.4 km, (c) 1 km and (d) 0.4 km. The parameter  $\delta_f$  is set to 3 km. Black arrows indicate the surface currents configuration at the beginning of the trajectories simulation. The radar current field has been sub-sampled (one vector every five grid nodes) for graphical readability.

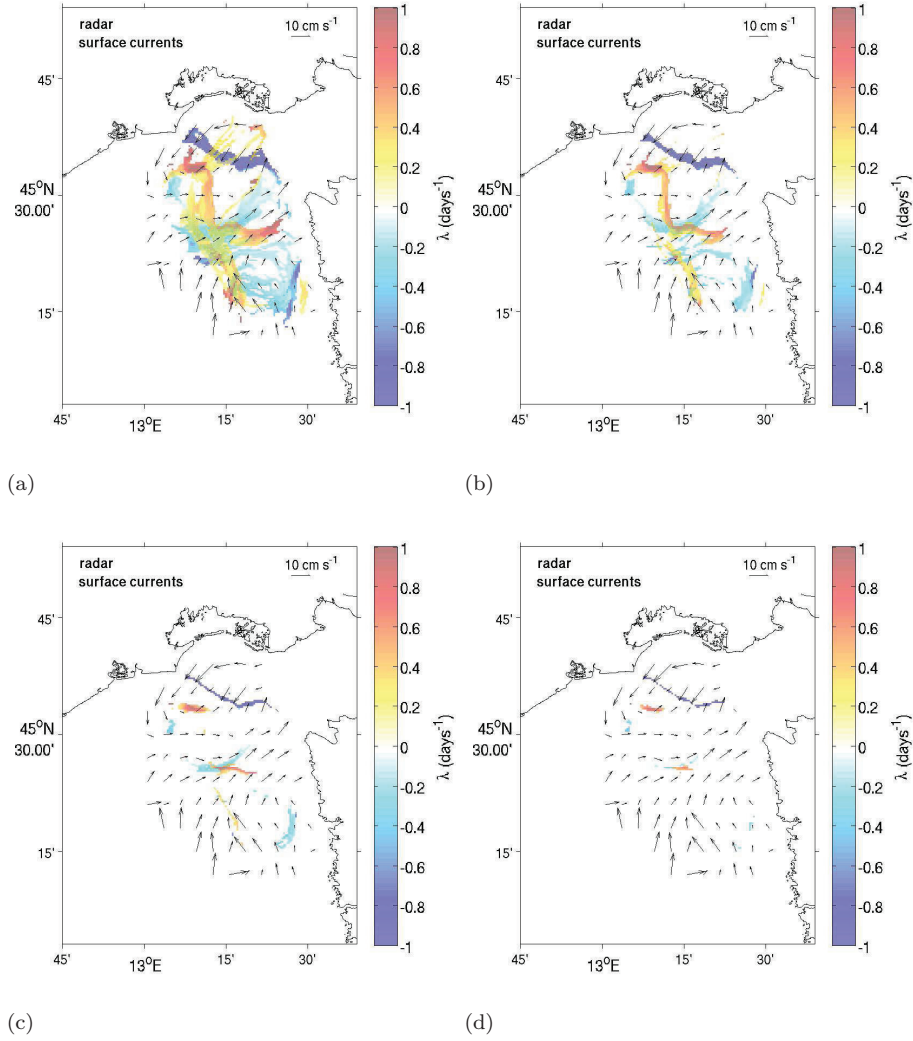


Figure 4: FSLE ( $\text{days}^{-1}$ ) trial maps for different  $\delta_f$ : (a) 1 km, (b) 1.6 km, (c) 3 km and (d) 5 km. The parameter  $\delta_i$  is set to 0.4 km. Black arrows indicate the surface currents configuration at the beginning of the trajectories simulation. The radar current field has been sub-sampled (one vector every five grid nodes) for graphical readability.

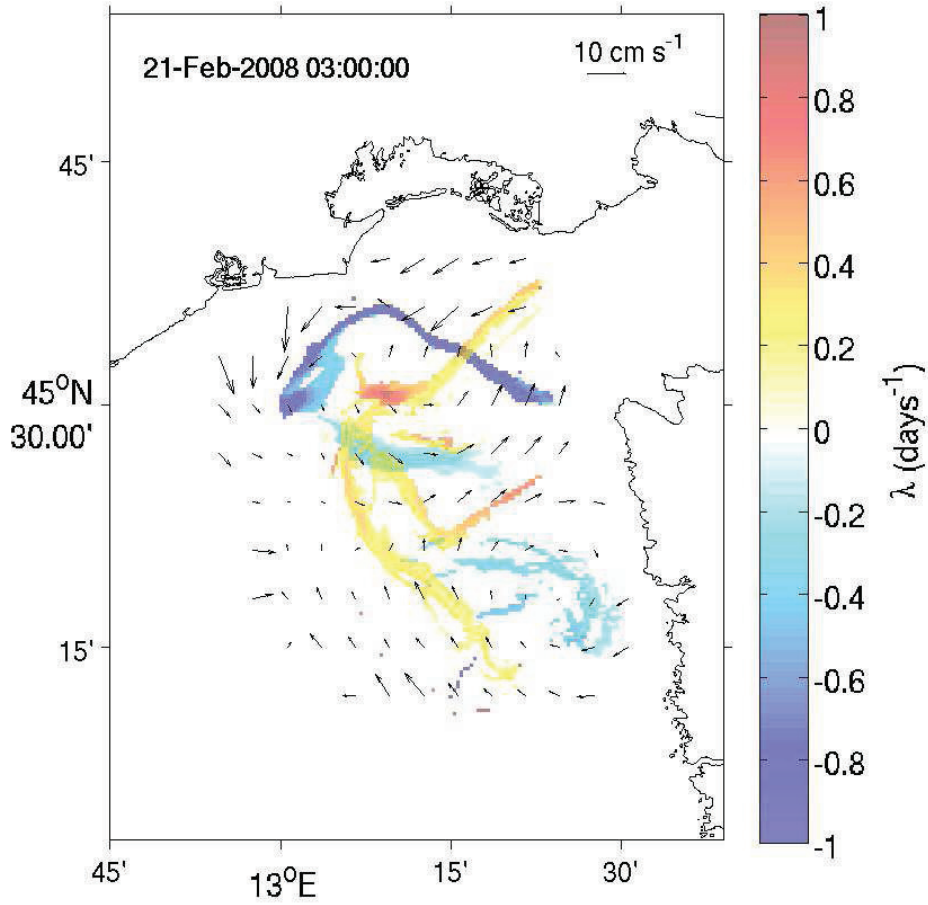
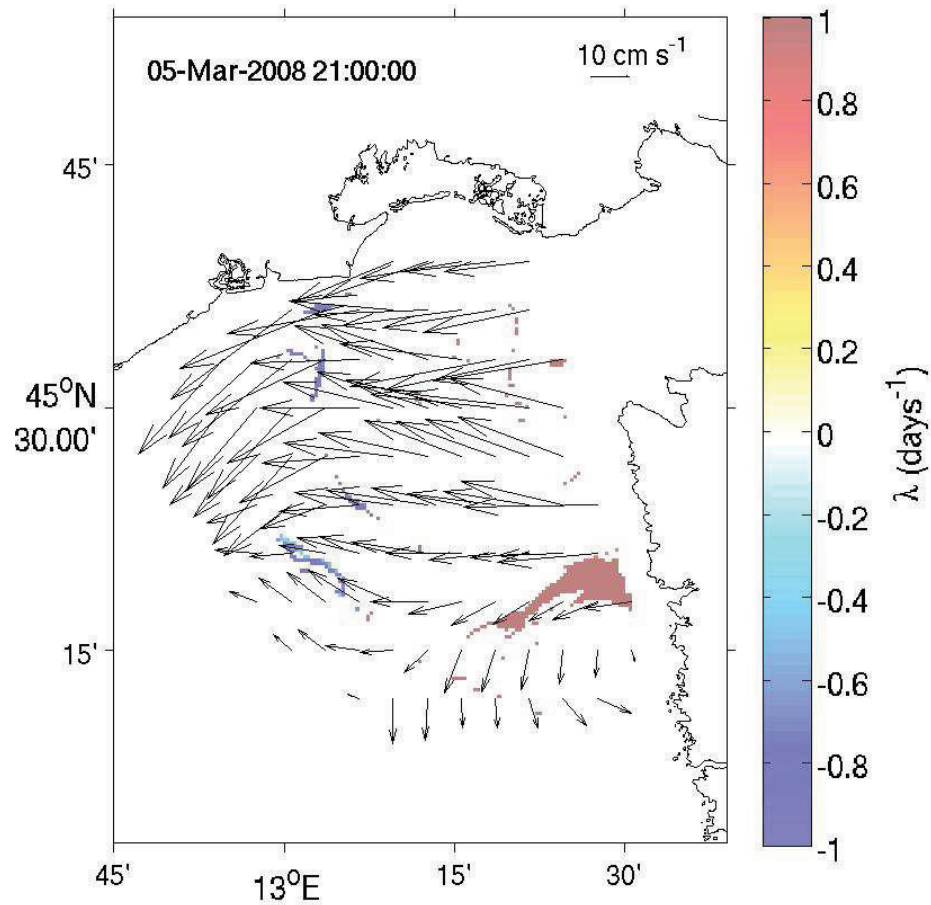
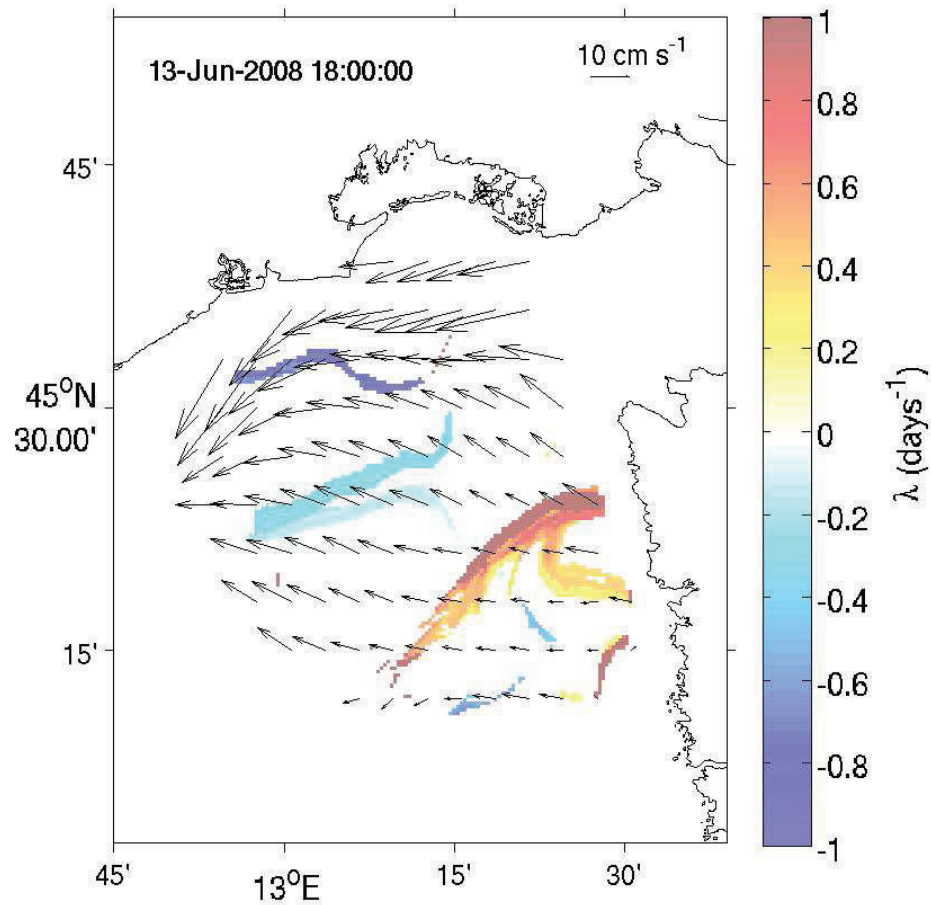


Figure 5: FSLE ( $\text{days}^{-1}$ ) map extracted from the calm wind period in February 2008. Black arrows indicate the mean surface current field during the calm wind period. The date specifies the beginning of the trajectories simulation. The radar current field has been sub-sampled (one vector every five grid nodes) for graphical readability.



(a)



(b)

Figure 6: FSLE (days<sup>-1</sup>) maps extracted from the Bora episodes: (a) in March 2008 and (b) in June 2008. Black arrows indicate the mean surface current field during the wind episode. The date specifies the beginning of the trajectories simulation. The radar current field has been sub-sampled (one vector every five grid nodes) for graphical readability.

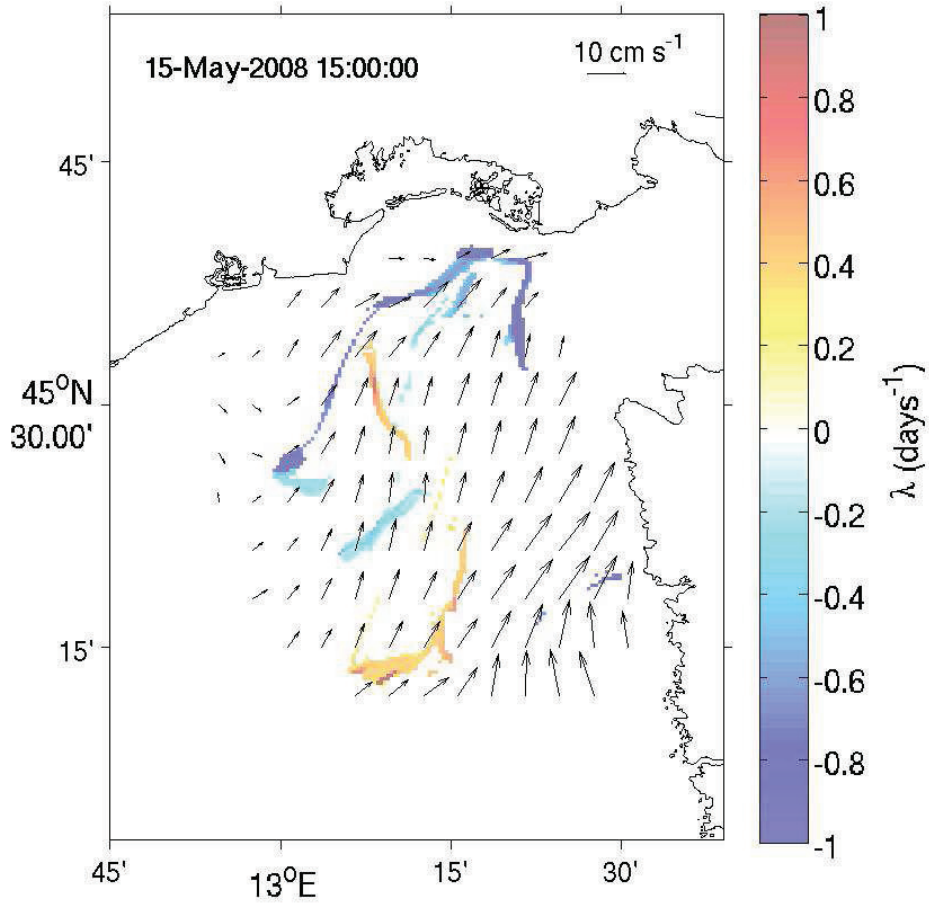


Figure 7: FSLE (days<sup>-1</sup>) map extracted from the Sirocco episode in May 2008. Black arrows indicate the mean surface current field during the wind episode. The date specifies the beginning of the trajectories simulation. The radar current field has been sub-sampled (one vector every five grid nodes) for graphical readability.



### RESEARCH HIGHLIGHTS

We study surface transport in NE Adriatic Sea associated with Bora and Sirocco wind

Application of the FSLE technique on the current fields detected by HF coastal radars

In calm wind conditions an attractive LCS crosses the GoT entrance (SE-NW direction)

In Bora episodes the attractive LCS is displaced westward, no barrier in front of GoT

In Sirocco cases the attractive LCS extends in SW-NE direction, for inflow in the GoT

1  
2  
3  
4  
5  
6  
7  
8  
9  
10  
11  
12  
13  
14  
15  
16  
17  
18  
19  
20  
21  
22  
23  
24  
25  
26  
27  
28  
29  
30  
31  
32  
33  
34  
35  
36  
37  
38  
39  
40  
41  
42  
43  
44  
45  
46  
47  
48  
49  
50  
51  
52  
53  
54  
55  
56  
57  
58  
59  
60  
61  
62  
63  
64  
65

## Surface transport in the Northeastern Adriatic Sea from FSLE analysis of HF radar measurements

Maristella Berta<sup>a,b,\*</sup>, Laura Ursella<sup>a</sup>, Francesco Nencioli<sup>c</sup>, Andrea M. Doglioli<sup>c</sup>,  
Anne A. Petrenko<sup>c</sup>, Simone Cosoli<sup>a</sup>

<sup>a</sup>*Istituto Nazionale di Oceanografia e di Geofisica sperimentale - OGS, Trieste, Italy*

<sup>b</sup>*University of Trieste, Trieste, Italy*

<sup>c</sup>*Aix-Marseille University, Mediterranean Institute of Oceanography (MIO), 13288,  
Marseille, Cedex 9, France ; Université du Sud Toulon-Var, CNRS-INSU/IRD UM 110*

---

### Abstract

This study focuses on the surface transport in the Northeastern Adriatic Sea and the related hydrodynamic connectivity with the Gulf of Trieste (GoT) under calm or typical wind conditions: Bora (from the NE) and Sirocco (from the SE). The surface transport in the area has been investigated by evaluating the Finite-Size Lyapunov Exponents (FSLE) on the current field measured by the High Frequency (HF) coastal radar network. FSLE allow to estimate Lagrangian Coherent Structures (LCSs), which provide information on the transport patterns associated with the flow and identify regions characterized by different dynamics. This work includes the development and set up of the FSLE algorithm applied for the first time to the specific Adriatic area considered. The FSLE analysis during calm wind reveals an attractive LCS crossing the GoT entrance, marking the convergence between the Northern Adriatic and the outflowing gulf waters. During Bora episodes this attractive LCS is displaced westward with respect to the calm wind case, indicating that Bora drives an extended coherent outflow from the GoT. On the other hand, Sirocco wind piles up the water along the northern end of the basin. In this area an attractive LCS is found, extending mainly in SW-NE direction. The sirocco-induced inflow of Adriatic waters in

---

\*CNR-ISMAR. Forte Santa Teresa, Pozzuolo di Lericci, 19032 (SP). Italy. Tel: (+39)0187-978316

*Email address:* maristella.bera@sp.ismar.cnr.it (Maristella Berta)

1  
2  
3  
4  
5  
6  
7  
8  
9 the GoT is mainly driven along its northern (Italian) side, as evidenced by the  
10 orientation of the LCS. Under Sirocco condition, as in Bora case, there is no  
11 barrier in front of the gulf. No relevant LCSs are observed in the southern radar  
12 coverage area except for Bora cases, when a repulsive LCS develops in front of  
13 the Istrian coast separating water masses to the North and the South of it.  
14  
15

16 *Keywords:* Adriatic Sea, Trieste Gulf, radar, surface transport, FSLE, LCS  
17  
18

---

19  
20 **1. Introduction**  
21

22 The Adriatic Sea is a basin of the Eastern Mediterranean Sea enclosed be-  
23 tween the Italian and the Balkan peninsula, and it separates respectively the  
24 Apennine mountains from the Dinaric Alps (Figure 1). It extends in the NW-  
25 SE direction and communicates with the Ionian Sea through the Otranto Strait,  
26 located at its southern end. The mean surface circulation of the Adriatic Sea  
27 is characterized by a northwestward flow along the Balkan coast, known as the  
28 Eastern Adriatic Current (EAC), and a southeastward flow along the Italian  
29 coast, called Western Adriatic Current (WAC) [Artegiani et al., 1997b; Zore,  
30 1956]. The EAC-WAC system results in a basin-wide cyclonic circulation in  
31 which three cyclonic gyres are embedded at the southern, middle and northern  
32 part of the Adriatic Sea, respectively [Artegiani et al., 1997a; Malanotte-Rizzoli  
33 and Bergamasco, 1983]. Observations of water mass properties and currents ev-  
34 idence that the Northern Adriatic circulation is strongly influenced by the winds  
35 over the Adriatic area [Poulain et al., 2001]. Due to its geographical orientation  
36 with respect to the surrounding orography (Apennines and Dinaric Alps) it is  
37 particularly affected by Bora and Sirocco winds [Orlić et al., 1994].  
38  
39

40 The Bora is a northeasterly cold and dry katabatic wind, with the most  
41 severe manifestations occurring typically during winter [Yoshino, 1976]. The  
42 Sirocco blows from S-SE and by crossing the Mediterranean Sea it gets warm  
43 and humid. Unlike the Bora, which is characterized by a gusty nature, it keeps  
44 more homogeneous spatial characteristics over the Adriatic Sea [Ferrarese et al.,  
45 2008].  
46  
47  
48  
49  
50  
51  
52  
53  
54  
55  
56  
57  
58  
59  
60  
61  
62  
63  
64  
65

1  
2  
3  
4  
5  
6  
7  
8  
9  
10  
11  
12  
13  
14  
15  
16  
17  
18  
19  
20  
21  
22  
23  
24  
25  
26  
27  
28  
29  
30  
31  
32  
33  
34  
35  
36  
37  
38  
39  
40  
41  
42  
43  
44  
45  
46  
47  
48  
49  
50  
51  
52  
53  
54  
55  
56  
57  
58  
59  
60  
61  
62  
63  
64  
65

24 In the Northern Adriatic area, the Bora drives several dynamical processes  
25 both at the surface and in the deeper layers. These include the dense water  
26 formation in the northern and central part, the latter compensated by strong  
27 upwelling along the eastern margin [Lazar et al., 2007; Orlić et al., 1992], and  
28 the intensification of the WAC [Ursella et al., 2006]. The most prominent Bora-  
29 induced feature is a double gyre circulation [Zore-Armanda and Gačić, 1987]  
30 developing as a consequence of the funneling of Bora to the North and the  
31 South of Istria (these paths are called “Bora corridors”) [Lazić and Tošić, 1998].  
32 This pattern has been identified both by drifters trajectories [Poulain, 2001] and  
33 by model simulations [Kuzmić et al., 2007; Jeffries and Lee, 2007]. On the other  
34 hand Sirocco enhances the EAC [Ursella et al., 2006] by piling up sea water  
35 along the Northern Adriatic coasts. Occasionally it can reverse the WAC along  
36 the Italian coastline, inducing a north-westward current particularly intense in  
37 the Northern part of the basin [Ferrarese et al., 2008; Kovačević et al., 2004].  
38 As a consequence, sea level rise is often observed in the region during Sirocco  
39 episodes [Orlić et al., 1994].

40 This study focuses on the northeastern area, which corresponds to the shal-  
41 low area of the basin and thus it is extremely sensitive to wind forcing and  
42 riverine inputs (Po, Tagliamento, Isonzo; Figure 1). For these reasons, surface  
43 currents in this part of the Adriatic Sea, have been continuously monitored by a  
44 coastal radar network in the framework of the NASCUM (North Adriatic Sur-  
45 face CUREnt Mapping) project. The surface currents in this area were analyzed  
46 by Mihanović et al. [2011] through the SOM (Self-Organizing Map) technique to  
47 identify the typical patterns developing for different wind conditions, with par-  
48 ticular emphasis on those associated with the prevailing wind regimes of Bora  
49 and Sirocco. The detected current patterns were indeed characterized by the  
50 expected circulation response, but, at the same time, they also evidenced new  
51 sub-mesoscale features never reported in previous studies.

52 The present study will focus on the eastern part of the Northern Adriatic,  
53 aiming in particular at investigating the surface transport and the related hy-  
54 drodynamic connectivity associated with the surface circulation between the

1  
2  
3  
4  
5  
6  
7  
8  
9 55 Gulf of Trieste (GoT) and the Northern Adriatic Sea under the typical wind  
10 56 conditions. The GoT is defined as the region of the Adriatic Sea North-East of  
11 57 the ideal line connecting Savudrija and Grado (Figure 1). According to Malačić  
12 58 and Petelin [2001] and Bogunović and Malačić [2009] the circulation in the GoT  
13 59 is driven by the EAC intrusion at intermediate depth along the southern side of  
14 60 the gulf. This induces GoT waters to follow the gulf coastline with a cyclonic  
15 61 pattern and then exit along the Italian margin. At the same time, a transversal  
16 62 outflow current develops at the surface crossing the GoT entrance from SE to  
17 63 NW [Malačić and Petelin, 2009].

23 64 The surface transport in the area will be investigated through the Finite-  
24 65 Size Lyapunov Exponent (FSLE) technique. This method allows to identify  
25 66 Lagrangian Coherent Structures (LCSs) on the basis of the relative dispersion  
26 67 between initially close particles. LCSs provide information on the transport  
27 68 patterns associated with the flow and they allow to identify regions character-  
28 69 ized by different dynamics [Ottino, 1989; d’Ovidio et al., 2004]. They indicate  
29 70 the directions along which water masses are advected by the flow; and, at the  
30 71 same time, the converging and diverging regions of the flow, since water masses  
31 72 are squeezed along attractive LCSs and stretched across repulsive ones. Finally,  
32 73 LCSs also represent transport barriers since they cannot be crossed by the ad-  
33 74 vected water masses. The FSLE method can be regarded as a complementary  
34 75 approach with respect to other Eulerian analysis usually applied to identify  
35 76 eddy’s core and to characterize mixing based on velocity field snapshots (such  
36 77 as vortex identification from eddy kinetic energy or Okubo-Weiss parameter).  
37 78 In fact FSLE maps depend on the spatio-temporal evolution of the velocity field  
38 79 and of its transport properties, and not only on the velocity configuration at a  
39 80 given scale and time [García-Olivares et al., 2007; d’Ovidio et al., 2009]. Since  
40 81 FSLE maps are computed through the integration of particle trajectories, they  
41 82 identify dynamical structures that organize the transport in a velocity field, with  
42 83 details below its original resolution and without any assumption on small scale  
43 84 dispersion features [Hernández-Carrasco et al., 2011]. This is possible because  
44 85 the integration of trajectories from an Eulerian velocity map to the next ones al-

1  
2  
3  
4  
5  
6  
7  
8  
9 86 lows to extract the information contained in the flow field temporal dependence,  
10 87 that on the other hand is lost when looking at each velocity map independently.  
11 88 Indeed, the trajectories of the synthetic particles advected in the surface current  
12 89 fields capture the smaller scale dynamics resulting from the variability of the  
13 90 mesoscale field.

14  
15  
16 91 In the Adriatic Sea, the FSLE method has been first used by Haza et al.  
17 92 [2007] to identify LCSs from NCOM (Navy Coastal Ocean Model) currents.  
18 93 Being based on a numerical model output, the comparison between the drifter  
19 94 trajectories and the identified LCSs corroborated the potential of integrating  
20 95 predictive coastal models with the FSLE method. A subsequent work by Haza  
21 96 et al. [2008] investigated the relative dispersion for the whole Adriatic Sea based  
22 97 on the NCOM model currents. The study showed that tracer dispersion is  
23 98 mainly controlled by large-scale circulation rather than by local regimes. This  
24 99 is in agreement with other studies based on open ocean LCSs derived from  
25 100 satellite velocity fields [Lehahn et al., 2007; d’Ovidio et al., 2009]. Nonetheless,  
26 101 a recent study by Nencioli et al. [2011] has shown that smaller scale processes,  
27 102 not resolved by large scale model or satellite data, are fundamental for studying  
28 103 transport patterns in coastal areas.

29  
30  
31 104 In terms of small scale processes, HF radars have a clear advantage over  
32 105 large scale models and satellite surveying, in that velocities measured by HF  
33 106 radar include processes over a broader range of spatial and temporal scales  
34 107 (from the submesoscale to larger scale circulation). For this reason, radar ve-  
35 108 locities are particularly suited for the analysis of coastal LCSs. This has been  
36 109 confirmed by the study performed in the Ligurian Sea by Haza et al. [2010],  
37 110 in which LCSs identified from VHF WERA radar current fields [Gurgel et al.,  
38 111 1999] were compared with the trajectories of drifter clusters. Although the LCS  
39 112 theory assumes 2D non-divergent flows, it was found that the motion of the  
40 113 surface drifters followed the VHF radar derived transport barriers, in spite of  
41 114 the presence of significant vertical velocities.

42  
43  
44 115 The present work represents the first development of an analogous FSLE  
45 116 technique applied to HF radar currents in the Adriatic Sea. This study aims at

1  
2  
3  
4  
5  
6  
7  
8  
9  
10  
11  
12  
13  
14  
15  
16  
17  
18  
19  
20  
21  
22  
23  
24  
25  
26  
27  
28  
29  
30  
31  
32  
33  
34  
35  
36  
37  
38  
39  
40  
41  
42  
43  
44  
45  
46  
47  
48  
49  
50  
51  
52  
53  
54  
55  
56  
57  
58  
59  
60  
61  
62  
63  
64  
65

117 determining transport patterns in the Northeastern Adriatic Sea during Bora  
118 and Sirocco events. This goal will be achieved by analyzing the high-resolution  
119 current measurements from the NASCUM radar network with the FSLE tech-  
120 nique. This work will also focus on several methodological aspects concerning  
121 the application of the FSLEs technique to radar datasets. This is particularly  
122 important since radar velocity fields are highly variable and cover smaller do-  
123 mains compared to satellite and numerical model fields used in previous studies.  
124 The sensitivity of the technique to different configurations of the FSLE param-  
125 eters will be discussed.

126 The paper is organized as follows: in Section 2 the datasets and the developed  
127 FSLE algorithm are described. Section 3 shows the results of the sensitivity  
128 analysis for different FSLE parameter settings and describes the LCSs maps  
129 obtained for different wind regimes. Finally, the discussion of results and the  
130 conclusions are presented in Section 4.

131 **2. Data and Methods**

132 *2.1. Wind episodes identification*

133 The FSLE analysis on sea surface currents is applied during periods charac-  
134 terized by strong, long-lasting events of Bora and Sirocco. In order to identify  
135 the most relevant wind episodes over the radar area, several datasets have been  
136 used, i.e. measured wind and sea level (SL) from different meteo-mareographic  
137 stations along the Northern Italian coast (Figure 1). The wind data in Tri-  
138 este, come from the meteo-oceanographic buoy, MAMBO-1, managed by OGS  
139 (*Istituto Nazionale di Oceanografia e di Geofisica Sperimentale*<sup>1</sup>). The wind  
140 time series in Venice are recorded at the Acqua Alta platform by ISMAR-CNR  
141 (*Istituto di Scienze Marine - Consiglio Nazionale delle Ricerche*<sup>2</sup>). While the  
142 SL time series are provided by ISPRA (*Istituto Superiore per la Ricerca e la*

---

<sup>1</sup><http://www.ogs.trieste.it/>

<sup>2</sup><http://www.ismar.cnr.it/>

1  
2  
3  
4  
5  
6  
7  
8  
9 143 *Protezione Ambientale*<sup>3</sup>).

10 144 The hourly wind data have been low-pass filtered (33 h LP) to remove  
11  
12 145 diurnal-period oscillations, associated with the sea-breeze regime [Cosoli et al.,  
13  
14 146 2012]. The same filter has been applied to the hourly SL series to remove tidal  
15  
16 147 harmonics and Adriatic seiches.

17 148 Bora events have been detected from the filtered wind time-series of the  
18  
19 149 Trieste station (Figure 2, upper panels). The episodes of Bora are defined when  
20  
21 150 at least 75% of the wind vectors, over a window of 3 days minimum, blow from  
22  
23 151 the first quadrant [i.e. between North and East, Ursella et al., 2006], with speed  
24  
25 152 greater than 5m/s.

26 153 The Sirocco events have been identified from the filtered wind data of the  
27  
28 154 Venice station (Figure 2, central panels). The episodes of strong Sirocco are  
29  
30 155 defined when at least 75% of the wind vectors, over a window of 3 days minimum,  
31  
32 156 blow from S-SE, with speed at least equal to 5m/s. Moreover, the effects of the  
33  
34 157 Sirocco occurrence have been identified from the tide-gauge measurements in  
35  
36 158 Venice station (Figure 2, bottom panel). In fact, the Sirocco piles up sea water  
37  
38 159 along the northernmost border of the Adriatic Sea, leading to the SL rise along  
39  
40 160 the northern Adriatic coast [Orlić et al., 1994]. A further contribution to the  
41  
42 161 SL rise may be also given by the large low atmospheric pressure structure with  
43  
44 162 weak horizontal pressure gradients, which however drives Sirocco itself [Poulain  
45  
46 163 and Raicich, 2001].

47 164 Calm wind periods have also been investigated as a term of comparison.  
48  
49 165 These are defined as periods of at least seven days with wind intensity lower  
50  
51 166 than 3 m/s.

52 167 The wind episodes are selected in the period limited to the widest available  
53  
54 168 radar coverage (February 2008 - August 2008, see Cosoli et al. [2012]). Such  
55  
56 169 conditions allow for better performances of the FSLE method, since particles  
57  
58 170 can be advected in a wider domain.

59 171 For each wind regime the most significant events have been selected in order

---

56 <sup>3</sup><http://www.mareografico.it/>



1  
2  
3  
4  
5  
6  
7  
8  
9 172 to evidence possible recurrent features in the detected LCSs. The identified  
10 173 wind events are summarized as follows (see Figure 2): the episodes of Bora of  
11 174 the 4-8 March 2008 and of Sirocco of the 14-18 May 2008, are the strongest  
12 175 wind manifestations for the entire period considered. These wind episodes were  
13 176 also identified by Mihanović et al. [2011] for describing the sea surface current  
14 177 patterns during typical wind episodes. An additional episode of weak Bora (12-  
15 178 15 June 2008) is shown for comparison with the strong Bora case. The longest  
16 179 calm wind period is found between 17-29 February 2008.

180 The different temporal length of these episodes does not affect the analysis  
181 since the particles, launched for the evaluation of the FSLE, are initialized in the  
182 period of interest, but their evolution is not forced to stop at the limits of this  
183 period. However, they can leave the velocity field according to the transport  
184 properties of the currents themselves.

185 The occurrence of these wind episodes has been further confirmed by high-  
186 resolution modeled wind fields coming from ALADIN/HR (*Aire Limitée Adap-*  
187 *tation dynamique Développement InterNational*), run by the Croatian Meteorolo-  
188 gical and Hydrological Service<sup>4</sup>. ALADIN/HR wind maps are available with  
189 2 km spatial resolution and 3 hours temporal resolution (not shown).

## 190 2.2. HF surface currents

191 The installed NASCUM network was composed of 3 CODAR (Coastal Ocean  
192 Dynamics Application Radar) Sea Sonde HF radar stations (dots in Figure 1),  
193 active from August 2007 to August 2008. Two stations were located along the  
194 Istrian coast (in Rt Zub and Savudrija) and the third one, included since De-  
195 cember 2007, on the Italian coast (in Bibione - Punta Tagliamento). The radars  
196 were set up in the 25 MHz frequency at 100 kHz bandwidth, allowing a range  
197 up to 50 km offshore with 1.5 km radial resolution and 5° angular resolution.  
198 Surface currents are mapped over a regular grid of about 30 km × 20 km (max-  
199 imum coverage) with 2 km spatial resolution and 1 h temporal resolution. The

---

<sup>4</sup>[http://meteo.hr/index\\_en.php/](http://meteo.hr/index_en.php/)

1  
2  
3  
4  
5  
6  
7  
8  
9  
200 current field covers the eastern and shallowest part of the Northern Adriatic  
201 with bottom depth from 20 m to 40 m, right in between the northern Bora  
202 “corridors” and directly affected by the Tagliamento river output (Figure 1).

203 The HF current dataset <sup>5</sup> comes from the processing of the raw radial mea-  
204 surements performed by Cosoli et al. [2012]. For more information about the  
205 treatment, the reader is referred to Chapman and Graber [1997] and Kovačević  
206 et al. [2004]. The current signal includes also the tidal component. Episodi-  
207 cally, current fields show some missing values at few points of the grid close to  
208 the baseline Bibione-Savudrija. This is due to the constraints in the intersect-  
209 ing beam geometry, required to minimize the effects of the site-to-site baseline  
210 instabilities. Therefore, a linear interpolation has been applied in order to com-  
211 plete the gap in the grid nodes to avoid the problem of truncated trajectories  
212 due to missing velocity values.

### 213 *2.3. FSLE application*

214 The FSLEs are evaluated by measuring the time needed for a particle pair  
215 to separate from an initial distance  $\delta_i$  to a final distance  $\delta_f$ . Thus, the analy-  
216 sis developed for this study includes two stages: first, the computation of the  
217 synthetic trajectories; second, the code which evaluates the FSLE and maps  
218 the final result. Particles trajectories are calculated by discretizing the advec-  
219 tion equation and applying the 4<sup>th</sup> order explicit Runge-Kutta method with a 4  
220 point bilinear interpolation [Hernández-Carrasco et al., 2011]. The values of  $\delta_i$   
221 and  $\delta_f$  influence the identification of the LCSs in the flow field, and depend on  
222 the characteristics of the flow field itself, on the length scale of the structures of  
223 interest and on the size of the domain. The initial distance affects the visibility  
224 of the details (the smaller  $\delta_i$ , the more details), as the resolution of the grid  
225 where the FLSEs are computed is chosen to be equal to the initial distance  
226 between particles [d’Ovidio et al., 2004; Lehahn et al., 2007]. This ensures that  
227 all the space in the velocity field is sampled once and just once. On the other

---

<sup>5</sup>[http://poseidon.ogs.trieste.it/jungo/NASCUM/index\\_en.html](http://poseidon.ogs.trieste.it/jungo/NASCUM/index_en.html)

1  
2  
3  
4  
5  
6  
7  
8  
9  
10  
11  
12  
13  
14  
15  
16  
17  
18  
19  
20  
21  
22  
23  
24  
25  
26  
27  
28  
29  
30  
31  
32  
33  
34  
35  
36  
37  
38  
39  
40  
41  
42  
43  
44  
45  
46  
47  
48  
49  
50  
51  
52  
53  
54  
55  
56  
57  
58  
59  
60  
61  
62  
63  
64  
65

228 hand, the final distance influences the detection of the structures (with larger  
229  $\delta_f$ , only the most stable and intense structures emerge).

230 Once these parameters are chosen, the FSLE are computed by launching an  
231 ensemble of synthetic particles over the FSLE grid and following the evolution of  
232 their relative distance. For each node of the FSLE grid, five particles are initial-  
233 ized with a central particle located over the grid node and the other four placed  
234 around it at a distance  $\delta_i$  along the latitudinal and longitudinal directions. This  
235 choice allows to account for the different intensity of dispersion along different  
236 directions [Boffetta et al., 2001] in order to retain the fastest diverging couples.  
237 FSLEs are computed every 3 hours using both forward and backward integra-  
238 tion in time, which allow to identify both the strongest repulsive and attractive  
239 LCSs during different wind regimes. Values of the FSLE  $\lambda$  are calculated at  
240 each node according to the definition [Sandulescu et al., 2007]:

241 • forward integration:

$$\lambda^+ = \frac{1}{\tau} \ln \frac{\delta_f}{\delta_i};$$

242 • backward integration:

$$\lambda^- = -\frac{1}{\tau} \ln \frac{\delta_f}{\delta_i};$$

243 where  $\tau$  is the time needed to separate two particles of the ensemble from  $\delta_i$   
244 up to  $\delta_f$ . The faster the divergence, the smaller is  $\tau$ , and the larger (in absolute  
245 value) is  $\lambda$ . It is important to remark, that divergence in backward integration  
246 actually identifies regions of convergence of the flow. If one of the particles of  
247 an ensemble leaves the velocity field before  $\delta_f$  is reached, then  $\lambda$  is not defined.  
248 Maximum values of the  $\lambda^+$  and  $\lambda^-$  fields identify repulsive and attractive LCSs,  
249 respectively. The maps in this paper present tangles of attractive and repulsive  
250 LCSs obtained by superposing both forward and backward integration FSLE  
251 fields [Molcard et al., 2006].

1  
2  
3  
4  
5  
6  
7  
8  
9 **3. Results**

10  
11 *3.1. FSLE method set up*

12  
13 The application of the FSLE algorithm to the radar current field requires  
14  
15 to set up the parameters defining initial and final separation distance between  
16  
17 particles,  $\delta_i$  and  $\delta_f$  respectively. Since there are no previous studies on FSLE  
18  
19 analysis in the Northeastern Adriatic Sea, an overview on the sensitivity analysis  
20  
21 performed on the  $\delta_i$  and  $\delta_f$  parameters for this particular case study is presented.

22  
23 In general, a suitable combination of the two parameters must be chosen. This  
24  
25 should take into account that although  $\delta_i$  can be fixed arbitrarily small, there  
26  
27 is an intrinsic limit on the details of the resulting structures which is associated  
28  
29 with the surface shear information captured in the current field itself. Fur-  
30  
31 thermore, if  $\delta_f$  is chosen larger than the separation distance achievable by the  
32  
33 particles advected within the finite spatial domain of HF radar velocities, no  
34  
35 structures will be detected from the flow field.

36  
37 Given the characteristics of the dataset and the focus of the present work,  
38  
39 we aim at identifying the transport structures associated with small-scale (i.e.  
40  
41 mesoscale) processes. The horizontal scale of mesoscale processes is represented  
42  
43 by the internal Rossby radius of deformation, which is about 3-5 km in the  
44  
45 Middle and Northern Adriatic [Masina and Pinardi, 1994]. However, eddies can  
46  
47 have even smaller size during winter when waters are completely mixed and  
48  
49 the first baroclinic Rossby radius of deformation almost vanishes [Bergamasco  
50  
51 et al., 1996]. Recent numerical findings from a climatic circulation model of  
52  
53 the northern Adriatic Sea confirm values around 3km in spring [Malačić et al.,  
54  
55 2012].

56  
57 In order to find a choice of parameters able to identify appropriately both  
58  
59 weak and strong LCSs during any of the wind regimes considered, several tests  
60  
61 for all the wind cases have been performed (not shown). The following results  
62  
63 are representative of calm wind, but are purposefully shown in order to evidence  
64  
65 how the characteristics of the FSLE field, and thus of the identified LCSs, change  
66  
67 depending on the chosen parameter values.

1  
2  
3  
4  
5  
6  
7  
8  
9  
10  
11  
12  
13  
14  
15  
16  
17  
18  
19  
20  
21  
22  
23  
24  
25  
26  
27  
28  
29  
30  
31  
32  
33  
34  
35  
36  
37  
38  
39  
40  
41  
42  
43  
44  
45  
46  
47  
48  
49  
50  
51  
52  
53  
54  
55  
56  
57  
58  
59  
60  
61  
62  
63  
64  
65

282 As a first trial, according to the value of the Rossby radius,  $\delta_f$  is fixed to 3  
283 km and several FSLE maps obtained for different  $\delta_i$  are compared (Figure 3).  
284 Starting from an initial distance between particles equal to the resolution of  
285 the radar velocity field (2 km) and successively reducing the parameter  $\delta_i$ , the  
286 detected LCSs keep their configuration while their features become sharper.  
287 This property of FSLE-based LCSs has been first recognized by Hernández-  
288 Carrasco et al. [2011], who identified it as fractal behavior. At the same time,  
289 it is important to remark that by reducing  $\delta_i$  the number of particles used in  
290 the analysis, and thus its computational requirements, increases. Considering  
291 the radar field resolution and the scales of interest,  $\delta_i=0.4$  km represents a good  
292 compromise between the FSLE map resolution and the computational efficiency  
293 to resolve structures within the range of few kilometers. Once the value of  $\delta_i$   
294 is set, an analysis on the sensitivity of the detected LCSs for different values  
295 of  $\delta_f$  is also performed. Since mesoscale ranges within less than 3 km up to  
296 about 5 km, different values of  $\delta_f$  were tested from 1 km to 5 km (Figure 4).  
297 Usually just a limited group of particle couples is able to reach the relative  
298 final distance chosen, depending on the spatial extension of the current field  
299 and on the surface shear caught by radar measurement. Moreover the greater  
300 the final distance is, the longer will be the time required for each couple to  
301 separate up to this value. Therefore for small  $\delta_f$  a lot of couples separate in  
302 very short time and the structures in the FSLE map are very broad and almost  
303 indistinguishable from one another, since they are detected also for very weak  
304 transport structures. On the other hand for large  $\delta_f$  fewer particles separate  
305 up to this value and the resulting structures are formed by only few points of  
306 the map. These are associated with the stronger, more persistent structures,  
307 which therefore are more relevant for characterizing the transport properties of  
308 the flow. This is true especially in strong wind cases (not shown) when currents  
309 are so strong and coherent in space that for  $\delta_f=3$  km all the particles leave the  
310 radar field before having reached the fixed final distance, so that the transport  
311 structures cannot be identified at all. In conclusion, the final distance which  
312 allows the identification of transport structures for any wind condition under

1  
2  
3  
4  
5  
6  
7  
8  
9 study is  $\delta_f=1.6$  km.

### 10 11 3.2. LCS patterns during wind episodes

12  
13 To investigate the changes in the LCS patterns with different wind condi-  
14 tions, several episodes for each wind regime have been analyzed and the most  
15 representative cases are presented in Figures 5 to 7. These maps show the  
16 FSLE field for a time centered within a given wind episode, to ensure that the  
17 dynamical conditions just before and after this period do not affect the tra-  
18 jectories evolution at the sea surface. In the figures, repulsive LCSs (FSLE  
19 maxima/separating trajectories) are in red, whereas attractive LCSs (FSLE  
20 minima/converging trajectories) are in blue.

21  
22 For the calm wind case in February the spatial configuration of the trans-  
23 port structures is quite broad and detailed (Figure 5). Several attractive and  
24 repulsive LCSs are identified and they cross each other within the radar ve-  
25 locity field. These transport structures evolve with a longer time scale (up to  
26 3-4 days), independently from the high temporal variability characterizing the  
27 velocity field (due to tidal oscillations in the diurnal and semidiurnal frequency  
28 bands and near-inertial oscillations, as observed by Cosoli et al. [2012]). This is  
29 a typical feature of LCSs since they result from the integration of trajectories  
30 over time scales much longer than the ones characterizing the variability of the  
31 velocity field.

32  
33 An attractive LCS is present in front of the Italian coast throughout the  
34 entire calm wind period. The structure marks the convergence between GoT  
35 and Northern Adriatic waters. Its eastern half is oriented South-East to North-  
36 West, as mean advection goes from the Istrian coast toward the river mouth  
37 of the Tagliamento. There, it forms a right angle with the Italian coastline  
38 direction, because the jet along the Italian coast is deviated by the fresh water  
39 output from the Tagliamento river. Cosoli et al. [2012] observed an analogous  
40 deviation of the surface currents in front of the Tagliamento estuary.

41  
42 A repulsive structure occupies the central part of the current field and crosses  
43 the attractive structure facing the entrance of the GoT and other weaker at-  
44  
45  
46  
47  
48  
49  
50  
51  
52  
53  
54  
55  
56  
57  
58  
59  
60  
61  
62  
63  
64  
65

1  
2  
3  
4  
5  
6  
7  
8  
9  
10  
11  
12  
13  
14  
15  
16  
17  
18  
19  
20  
21  
22  
23  
24  
25  
26  
27  
28  
29  
30  
31  
32  
33  
34  
35  
36  
37  
38  
39  
40  
41  
42  
43  
44  
45  
46  
47  
48  
49  
50  
51  
52  
53  
54  
55  
56  
57  
58  
59  
60  
61  
62  
63  
64  
65

343 tractive structures in the field. The attractive structure to the south-east of the  
344 radar field is associated to an anticyclonic vortex in front of the Istrian coast.  
345 The current field presents several patterns with length scale larger than the  
346 internal Rossby radius of deformation identified by Masina and Pinardi [1994].  
347 The mesoscale length and variability also depends on stratification conditions  
348 and can be several times smaller/bigger than the internal radius of deformation  
349 (about 5km), as observed also by Bergamasco et al. [1996]. For this reason, in  
350 order to compare this case to the other wind episodes, the analysis will focus on  
351 the pattern that can be considered recurrent, that is the strongest attractive fil-  
352 ament at the entrance of GoT, related to the water exchange between the North  
353 Adriatic and the gulf itself (process already observed in the seasonal mesoscale  
354 study by Malačić and Petelin [2009]).

355 The FSLE analysis in the Bora case focuses on the March episode (Fig-  
356 ure 6(a)). Before and after the Bora event, wind conditions are predominantly  
357 calm and the spatial organization of LCSs is similar to the calm case of February  
358 just described. The response of the surface current to Bora wind is almost in-  
359 stantaneous, showing the development of intense westward/south-westward cur-  
360 rents throughout the radar domain. This is in agreement with the observations  
361 from Cosoli et al. [2012]; Malačić et al. [2012]; Mihanović et al. [2011]. Along  
362 the Istrian coastline, these currents are weaker than the ones further north. The  
363 resulting meridional current shear reflects the wind pattern over this part of the  
364 Adriatic basin: Bora is stronger along the northern “corridor”, and weaker to  
365 the south where it is screened by coastal orography. This north-south current  
366 shear introduces cyclonic vorticity extending far off from the Istrian coast, as  
367 already observed by Cosoli et al. [2012].

368 The evolution of the LCSs during Bora cases is characterized by a sequence of  
369 recurrent patterns: at the beginning of the Bora episode the attractive LCS typ-  
370 ical of calm wind conditions (Figure 5) is still present in the northernmost part  
371 of the radar domain in front of the Italian coastline. The structure remains sta-  
372 ble until the Bora has fully developed (not shown), but it is not present anymore  
373 as soon as the westward current pattern extends over the whole Northeastern

1  
2  
3  
4  
5  
6  
7  
8  
9 374 Adriatic (Figure 6(a)).

10 375 The disappearance of this attractive transport structure during Bora episodes,  
11  
12 376 and its reappearance as soon as Bora ceases, indicates that the LCS does not  
13  
14 377 vanishes but it is just displaced westward outside the radar domain by the pres-  
15  
16 378 ence of the intense, homogeneous Bora-driven currents. This can be evidenced  
17  
18 379 through the analysis of an episode of weak Bora, such as the one identified in  
19  
20 380 June 2008 (Figure 6(b)). The initial evolution of the transport structures is  
21  
22 381 analogous to the strongest Bora case already analyzed. In fact, at the begin-  
23  
24 382 ning of the Bora episode an attractive LCS is present to the north of the radar  
25  
26 383 domain. However, during such event, the Bora-driven westward currents are less  
27  
28 384 homogeneous over the basin, so that the region of convergence is still present in  
29  
30 385 front of the Italian coast.

31 386 The development of a repulsive LCS in front of the Istrian coast is another  
32  
33 387 common feature of both strong and weak Bora episodes. However, during the  
34  
35 388 weaker events, this LCS is less intense but more extended than the one devel-  
36  
37 389 oping during the strong ones.

38 390 The FSLE analysis in case of Sirocco forcing focuses on the event in May 2008  
39  
40 391 (Figure 7). Regardless of the currents configuration before a Sirocco event, as  
41  
42 392 soon as Sirocco starts to blow it induces an homogeneous north-northeastward  
43  
44 393 current. After the Sirocco has reached a steady state, this uniform current,  
45  
46 394 developed throughout all the radar field, induces the piling up of surface waters  
47  
48 395 in the northern part of the basin. A part of this water mass converges where  
49  
50 396 the attractive LCS is found, stretched from SW to NE, and enters the GoT  
51  
52 397 mostly along the northern (Italian) coastline. The intensified inflow along the  
53  
54 398 northern side of the GoT is also supported by recent numerical model findings  
55  
56 399 [Malačić et al., 2012]. The transport associated with this LCS is from West to  
57  
58 400 East, which is reversed with respect to the calm wind case when waters flow  
59  
60 401 cyclonically following the basin coastline. On the other hand, the meridional  
61  
62 402 part of the flow field does not show intense structures, since the currents are  
63  
64 403 rather uniform in direction and intensity and the advected particles do not  
65 404 experience the shear necessary to diverge or converge. When Sirocco relaxes



1  
2  
3  
4  
5  
6  
7  
8  
9  
10  
11  
12  
13  
14  
15  
16  
17  
18  
19  
20  
21  
22  
23  
24  
25  
26  
27  
28  
29  
30  
31  
32  
33  
34  
35  
36  
37  
38  
39  
40  
41  
42  
43  
44  
45  
46  
47  
48  
49  
50  
51  
52  
53  
54  
55  
56  
57  
58  
59  
60  
61  
62  
63  
64  
65

405 the cyclonic gyre is gradually restored so that the eastward current along Italy  
406 returns and the transport associated to the attractive LCS reverses back in  
407 westward direction (not shown).

408 **4. Discussion and conclusions**

409 The surface transport in the Northeastern Adriatic Sea has been investigated  
410 by applying the FSLE technique on the current field detected by the HF coastal  
411 radar network active in the period from August 2007 to August 2008. The anal-  
412 ysis is limited to the period from February to August 2008, when the spatial  
413 coverage of radar measurements was maximized under the three-site configura-  
414 tion. The interest is focused on the surface dynamics of this area associated with  
415 the typical wind regimes, Bora and Sirocco, compared to calm wind. Previous  
416 studies [d’Ovidio et al., 2009; García-Olivares et al., 2007] have confirmed the  
417 advantage of using the FSLE technique over more traditional Eulerian diagnos-  
418 tics for detecting the transport structures which separate dynamically distinct  
419 regions of a flow. Moreover, compared to other Lagrangian diagnostics, such  
420 as the analysis of sparse drifter trajectories, the FSLE technique allows to re-  
421 trieve information over broader domains, and thus is better suited for studies  
422 at the regional scale. Being the very first time that FSLE technique is applied  
423 to HF radar current fields of the Northern Adriatic Sea, it has been of crucial  
424 importance to investigate the sensitivity of the FSLE analysis with respect to  
425 the key parameters (initial distance,  $\delta_i$ , and final separation distance of parti-  
426 cles,  $\delta_f$ ) that control structures coverage and details visibility. Despite the very  
427 high variability of the radar current fields, the reasonably chosen values of these  
428 parameters has allowed to identify and investigate the evolution of the strongest  
429 transport structures.

430 In summary, the FSLE analysis on the current field revealed the presence of  
431 recurrent surface transport structures during the different wind regimes consid-  
432 ered (calm period, Bora and Sirocco). The current field during the calm wind  
433 period is characterized by the presence of multiple structures. Their persistence

1  
2  
3  
4  
5  
6  
7  
8  
9  
10  
11  
12  
13  
14  
15  
16  
17  
18  
19  
20  
21  
22  
23  
24  
25  
26  
27  
28  
29  
30  
31  
32  
33  
34  
35  
36  
37  
38  
39  
40  
41  
42  
43  
44  
45  
46  
47  
48  
49  
50  
51  
52  
53  
54  
55  
56  
57  
58  
59  
60  
61  
62  
63  
64  
65

434 in time is longer when compared to the other wind cases analyzed. An attractive  
435 LCS crosses the GoT entrance where the gulf and the North Adriatic waters  
436 converge. A repulsive structure is present in the central part of the radar field.  
437 The transport structures identified in strong Bora episodes show the displace-  
438 ment of the attractive LCS from the GoT entrance further west. Moreover a  
439 repulsive structure develops in front of the Istrian coast. On the other hand,  
440 during Sirocco events an attractive structure is present along the Italian coast.  
441 The transport associated with this LCS is from west to east, opposite to the  
442 calm wind case. This LCS indicates that Adriatic waters pile up along the  
443 northern coast.

444 As already pointed out, the surface circulation of the GoT is characterized  
445 by an outflowing transversal current developing from its southern border to the  
446 Tagliamento estuary, that merges with the westward flow along the Italian coast  
447 [Malačić and Petelin, 2009]. This FSLE analysis identifies an attractive LCS  
448 in front of the GoT entrance, which is associated with the transport driven  
449 by this transversal current out of the GoT. This structure is present in all the  
450 considered wind regimes but its location with respect to the Italian coast and  
451 the direction of transport associated with it varies.

452 During calm wind periods the attractive LCS extends from the northern  
453 Istrian tip to the Tagliamento river and further west, representing the barrier  
454 to the outflow of GoT waters to the Northern Adriatic Sea. The advection  
455 associated with this LCS is westward, in agreement with the diagonal current  
456 pattern typical of the GoT: surface waters entering the gulf along the Istrian  
457 coast and exiting from the Italian side of the GoT in a cyclonic pattern [Malačić  
458 and Petelin, 2001].

459 During weak Bora events, the attractive LCS is displaced westward with  
460 respect to its position in calm wind periods. The spatial configuration of this  
461 LCS with respect to the gulf entrance shows the location where the GoT surface  
462 waters extends to meet the Northern Adriatic coastal flow. On the other hand  
463 during strong Bora events there is no more evidence of the attractive LCS in  
464 the radar field, indicating that the convergence area, and thus the boundary of

1  
2  
3  
4  
5  
6  
7  
8  
9  
10  
11  
12  
13  
14  
15  
16  
17  
18  
19  
20  
21  
22  
23  
24  
25  
26  
27  
28  
29  
30  
31  
32  
33  
34  
35  
36  
37  
38  
39  
40  
41  
42  
43  
44  
45  
46  
47  
48  
49  
50  
51  
52  
53  
54  
55  
56  
57  
58  
59  
60  
61  
62  
63  
64  
65

465 westward outflow from the GoT, could be positioned beyond the western limit  
466 of the radar domain. A spatially coherent outflow from the GoT can indeed  
467 be observed from the radar measurements. This is in agreement with Malačić  
468 and Petelin [2009], who observed a similar outflow in response of intense wind  
469 forcing, and with Mihanović et al. [2011] who observed that Bora drives a sea  
470 level decrease in Trieste and, at the same time, a sea level rise in Venice.

471 To accurately identify the outflow barrier during strong Bora episodes, a  
472 wider current field would be necessary, either by extending westward the radar  
473 network or by using modeled current fields. In either weak and strong Bora cases  
474 a repulsive LCS develops in front of the Istrian coast. This structure represents  
475 a real transport barrier for the water masses present to the north and south of  
476 it. Any surface tracer present to the south of this repulsive LCS will not cross  
477 it and, therefore, the northward flow along the coast, characteristic of calm  
478 wind conditions, is temporarily halted. This determines a reduced connectivity  
479 between the Istrian coast and the GoT. This LCS could represent the southern  
480 boundary of the northern jet current exiting from the GoT and developing as a  
481 consequence of the Bora funneling between Dinaric Alps.

482 During Sirocco episodes the position of the attractive structure is found  
483 northeastward, as a consequence of the piling up of waters along the northern  
484 Adriatic coasts. Therefore there is no transport barrier in front of the GoT,  
485 indicating the occurrence of an extended inflow of North Adriatic waters into  
486 the GoT. Such inflow in the gulf is also confirmed by the observed sea level rise  
487 in Trieste during analogous wind events [Mihanović et al., 2011]. In this case,  
488 the local transport along this LCS is from west to east, and not in the opposite  
489 direction as during the typical cyclonic circulation of the North Adriatic area.  
490 The SW-NE orientation of the attractive LCS might indicate that the inflow  
491 comes from the open Adriatic rather than from coastal regions.

492 The application of the FSLE method on HF radar currents in the Northeast-  
493 ern Adriatic area can provide important information about horizontal transport  
494 dynamics. Such information could be greatly improved with the further devel-  
495 opment of a network of observation in the Northern Adriatic, which could lead

1  
2  
3  
4  
5  
6  
7  
8  
9  
10  
11  
12  
13  
14  
15  
16  
17  
18  
19  
20  
21  
22  
23  
24  
25  
26  
27  
28  
29  
30  
31  
32  
33  
34  
35  
36  
37  
38  
39  
40  
41  
42  
43  
44  
45  
46  
47  
48  
49  
50  
51  
52  
53  
54  
55  
56  
57  
58  
59  
60  
61  
62  
63  
64  
65

496 to more refined transport analysis.

497       Concerning potential applications of the FSLE method, it could be directly  
498 used in case of sea accidents or pollutant discharge to identify the possible path-  
499 ways of dispersion from reliable near-real time velocity fields. This will allow  
500 to identify the potential source area of the pollutant, and will provide a crucial  
501 information to circumscribe the intervention area and guide the emergency op-  
502 erations.

503

### *Acknowledgements*

The authors thank OGS, ISMAR-CNR and ISPRA for providing wind and sea level time series. The authors are grateful to Dr. Miroslav Gačić for supporting this work and for the stimulating discussion about the interpretation of the results. Gratitude is due to Dr. Annalisa Griffa for the precious suggestions during the development of the FSLE algorithm. Maristella Berta thanks MIO for the hospitality and financial support during her stay in Marseille for the advancement of scientific research. Maristella Berta shows her appreciation to Dr. Angélique Haza for sharing with the authors her experienced opinion about the results of this work.

### **References**

### **References**

Artegiani, A., Bregant, D., Paschini, E., Pinardi, N., Raicich, F., Russo, A.,  
1997a. The Adriatic Sea general circulation. Part II: baroclinic circulation  
structure. *J. Phys. Oceanogr.* 27, 1515–1532.

Artegiani, A., Bregant, D., Paschini, E., Pinardi, N., Raicich, F., Russo, A.,  
1997b. The Adriatic Sea general circulation. Part I: air-sea interactions and  
water masses structure. *J. Phys. Oceanogr.* 27, 1492–1514.

- 1  
2  
3  
4  
5  
6  
7  
8  
9 Bergamasco, A., Gačić, M., Boscolo, R., Umgiesser, G., 1996. Winter oceanographic conditions and water masses balance in the Northern Adriatic (February 1993). *J. Marine Syst.* 7, 67–94.
- 10  
11  
12  
13  
14 Boffetta, G., Lacorata, G., Redaelli, G., Vulpiani, A., 2001. Detecting barriers  
15 to transport: a review of different techniques. *Physica D* 159, 58–70.
- 16  
17  
18 Bogunović, B., Malačić, V., 2009. Circulation in the Gulf of Trieste:  
19 measurements and model results. *Il Nuovo Cimento (C)* 31, 301–326.  
20 Doi:10.1393/ncc/i2008-10310-9.
- 21  
22  
23 Chapman, R., Graber, H., 1997. Validation of (HF) radar measurements.  
24 *Oceanography* 10, 76–79.
- 25  
26  
27 Cosoli, S., Gačić, M., Mazzoldi, A., 2012. Surface current variability and wind  
28 influence in the Northern Adriatic Sea as observed from High-Frequency (HF)  
29 radar measurements. *Cont. Shelf Res.* 33, 1–13.
- 30  
31  
32  
33 d’Ovidio, F., Fernández, V., Hernández-García, E., López, C., 2004. Mixing  
34 structures in the Mediterranean Sea from Finite-Size Lyapunov Exponents.  
35 *Geophys. Res. Lett.* 31.
- 36  
37  
38 d’Ovidio, F., Isern-Fontanet, J., López, C., Hernández-García, E., García-  
39 Ladona, E., 2009. Comparison between Eulerian diagnostics and finite-size  
40 Lyapunov exponents computed from altimetry in the Algerian basin. *Deep-  
41 Sea Res. I* 56, 15–31.
- 42  
43  
44  
45 Ferrarese, S., Cassardo, C., Elmi, A., Genovese, R., Longhetto, A., Manfrin, M.,  
46 Richiardone, R., 2008. Response of temperature and sea surface circulation  
47 to a Sirocco wind event in the Adriatic basin: a model simulation. *J. Marine  
48 Syst.* 74, 659–671.
- 49  
50  
51  
52 García-Olivares, A., Isern-Fontanet, J., García-Ladona, E., 2007. Dispersion of  
53 passive tracers and finite-scale Lyapunov exponents in the Western Mediter-  
54 ranean Sea. *Deep-Sea Res. I* 54, 253–268.
- 55  
56  
57  
58  
59  
60  
61  
62  
63  
64  
65

- 1  
2  
3  
4  
5  
6  
7  
8  
9 Gurgel, K.W., Antonischski, G., Essen, H.H., Schlick, T., 1999. Wellen radar  
10 (WERA): a new ground-wave hf radar for ocean remote sensing. *Coast. Eng.*  
11 37, 219–234.  
12  
13  
14 Haza, A.C., Griffa, A., Martin, P., Molcard, A., Ozgokmen, T.M., Poje, A.C.,  
15 Barbanti, R., Book, J.W., Poulain, P.M., Rixen, M., Zanasca, P., 2007.  
16 Model-based directed drifter launches in the Adriatic Sea: results from the  
17 DART experiment. *Geophys. Res. Lett.* 34.  
18  
19  
20  
21 Haza, A.C., Ozgokmen, T.M., Griffa, A., Molcard, A., Poulain, P.M., Peggion,  
22 G., 2010. Transport dispersion processes in small-scale coastal flows: relative  
23 dispersion from VHF radar measurements in the Gulf of La Spezia. *Ocean*  
24 *Dynam.* 60, 861–882.  
25  
26  
27  
28 Haza, A.C., Poje, A.C., Ozgokmen, T.M., Martin, P., 2008. Relative dispersion  
29 from a high-resolution coastal model of the Adriatic Sea. *Ocean Model.* 22,  
30 48–65.  
31  
32  
33  
34 Hernández-Carrasco, I., López, C., Hernández-García, E., Turiel, A., 2011. How  
35 reliable are finite-size Lyapunov exponents for the assessment of ocean dy-  
36 nam.? *Ocean Model.* 36, 208–218.  
37  
38  
39 Jeffries, M.A., Lee, C.M., 2007. A climatology of the northern Adriatic Sea’s  
40 response to bora and river forcing. *J. Geophys. Res.* 112.  
41  
42  
43 Kovačević, V., Gačić, M., Mancero Mosquera, I., Mazzoldi, A., Marinetti, S.,  
44 2004. HF radar observation in the Northern Adriatic: surface current field in  
45 front of the Venetian Lagoon. *J. Marine Syst.* 51, 95–122.  
46  
47  
48  
49 Kuzmić, M., Janeković, I., Book, J.W., Martin, P.J., Doyle, J.D., 2007. Model-  
50 ing the northern Adriatic double-gyre response to intense bora wind: a revisit.  
51 *J. Geophys. Res.* 112. Doi:10.1029/2005JC003377.  
52  
53  
54 Lazar, M., Pavić, M., Pasarić, Z., Orlić, M., 2007. Analytical modelling of  
55 wintertime coastal jets in the Adriatic Sea. *Cont. Shelf Res.* 27, 275–285.  
56  
57  
58

- 1  
2  
3  
4  
5  
6  
7  
8  
9 Lazić, L., Tošić, I., 1998. A real data simulation of the Adriatic Bora and the  
10 impact of mountain height on the Bora trajectories. *Meteorol. Atmos. Phys.*  
11 66, 143–155.  
12  
13  
14 Lehahn, Y., d’Ovidio, F., Lévy, M., Heifetz, E., 2007. Stirring of the northeast  
15 Atlantic spring bloom: a Lagrangian analysis based on multisatellite data. *J.*  
16 *Geophys. Res.* 112.  
17  
18  
19 Malanotte-Rizzoli, P., Bergamasco, A., 1983. The dynamics of the coastal region  
20 of the Northern Adriatic Sea. *J. Phys. Oceanogr.* 13, 1105–1130.  
21  
22  
23 Malačić, V., Petelin, B., 2001. Regional studies. The gulf of Trieste., in:  
24 Cushman-Roisin, B., Gačić, M., Poulain, P.M., Artegiani, A. (Eds.), *Physical*  
25 *oceanography of the Adriatic Sea: past, present and future.* Kluwer Academic  
26 Publishers.  
27  
28  
29 Malačić, V., Petelin, B., 2009. Climatic circulation in the Gulf of Trieste (north-  
30 ern Adriatic). *J. Geophys. Res.* 114. Doi:10.1029/2008JC004904.  
31  
32  
33 Malačić, V., Petelin, B., Vodopivec, M., 2012. Topographic control of  
34 wind-driven circulation in the northern Adriatic. *J. Geophys. Res.* 117.  
35 Doi:10.1029/2012JC008063.  
36  
37  
38  
39 Masina, S., Pinardi, N., 1994. Mesoscale data assimilation studies in the middle  
40 Adriatic Sea. *Cont. Shelf Res.* 14, 1293–1310.  
41  
42  
43  
44 Mihanović, H., Cosoli, S., Vilibić, I., Ivanković, D., Dadić, V., Gačić, M.,  
45 2011. Surface current patterns in the northern Adriatic extracted from high-  
46 frequency radar data using self-organizing map analysis. *J. Geophys. Res.*  
47 116. Doi:10.1029/2011JC007104.  
48  
49  
50  
51 Molcard, A., Poje, A.C., Ozgokmen, T.M., 2006. Directed drifter launch strate-  
52 gies for Lagrangian data assimilation using hyperbolic trajectories. *Ocean*  
53 *Model.* 12, 268–289.  
54  
55  
56  
57  
58  
59  
60  
61  
62  
63  
64  
65

- 1  
2  
3  
4  
5  
6  
7  
8  
9 Nencioli, F., d'Ovidio, F., Doglioli, A.M., Petrenko, A.A., 2011. Surface coastal  
10 circulation patterns by in-situ detection of Lagrangian Coherent Structures.  
11 Geophys. Res. Lett. 38. Doi:10.1029/2011GL048815.  
12  
13  
14 Orlić, M., Gačić, M., La Violette, P.E., 1992. The currents and circulation of  
15 the Adriatic Sea. *Oceanol. Acta* 15, 109–124.  
16  
17  
18 Orlić, M., Kuzmić, M., Pasarić, Z., 1994. Response of the Adriatic Sea to the  
19 Bora and Sirocco forcing. *Cont. Shelf Res.* 14, 91–116.  
20  
21  
22 Ottino, J.M., 1989. *The kinematics of mixing: stretching, chaos and transport.*  
23 Cambridge University Press.  
24  
25  
26 Poulain, P.M., 2001. Adriatic Sea surface circulation as derived from drifter  
27 data between 1990 and 1999. *J. Marine Syst.* 29, 3–32.  
28  
29  
30 Poulain, P.M., Kourafalou, V.H., Cushman-Roisin, B., 2001. Northern Adriatic  
31 Sea, in: Cushman-Roisin, B., Gačić, M., Poulain, P.M., Artegiani, A. (Eds.),  
32 *Physical oceanography of the Adriatic Sea: past, present and future.* Kluwer  
33 Academic Publishers.  
34  
35  
36  
37 Poulain, P.M., Raicich, F., 2001. Forcings, in: Cushman-Roisin, B., Gačić, M.,  
38 Poulain, P.M., Artegiani, A. (Eds.), *Physical oceanography of the Adriatic*  
39 *Sea: past, present and future.* Kluwer Academic Publishers.  
40  
41  
42 Sandulescu, M., López, C., Hernández-García, E., Feudel, U., 2007. Plankton  
43 blooms in vortices: the role of biological and hydrodynamic timescales.  
44 *Nonlinear Proc. Geoph.* 14, 443–454.  
45  
46  
47  
48 Ursella, L., Poulain, P.M., Signell, R.P., 2006. Surface drifter derived circulation  
49 in the northern and middle Adriatic Sea: response to wind regime and season.  
50 *J. Geophys. Res.* 111. [printed 112(C3),2007].  
51  
52  
53 Yoshino, M.M., 1976. *Local wind Bora.* University of Tokyo Press.  
54  
55  
56 Zore, M., 1956. On gradient currents in the Adriatic Sea. *Acta Adriat.* 8, 1–38.  
57  
58  
59  
60  
61  
62  
63  
64  
65



1  
2  
3  
4  
5  
6  
7  
8  
9 Zore-Armanda, M., Gačić, M., 1987. Effect of Bura on the circulation in the  
10 Northern Adriatic. Ann. Geophys. 5B, 93-102.  
11  
12  
13  
14  
15  
16  
17  
18  
19  
20  
21  
22  
23  
24  
25  
26  
27  
28  
29  
30  
31  
32  
33  
34  
35  
36  
37  
38  
39  
40  
41  
42  
43  
44  
45  
46  
47  
48  
49  
50  
51  
52  
53  
54  
55  
56  
57  
58  
59  
60  
61  
62  
63  
64  
65

1  
2  
3  
4  
5  
6  
7  
8  
9  
10  
11  
12  
13  
14  
15  
16  
17  
18  
19  
20  
21  
22  
23  
24  
25  
26  
27  
28  
29  
30  
31  
32  
33  
34  
35  
36  
37  
38  
39  
40  
41  
42  
43  
44  
45  
46  
47  
48  
49  
50  
51  
52  
53  
54  
55  
56  
57  
58  
59  
60  
61  
62  
63  
64  
65

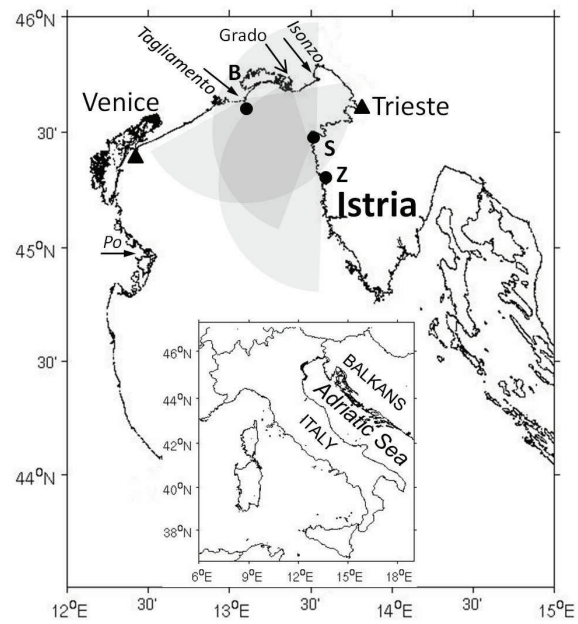


Figure 1: The data set coverage over the Northern Adriatic area with the radar stations (dots) in Bibione (B), Savudrija (S) and Rt Zub (Z). The meteo-mareographic stations in Trieste and Venice (triangles). The main river estuaries: Po, Tagliamento and Isonzo. The Gulf of Trieste is the sea area landlocked within Savudrija-Grado ideal baseline.

1  
2  
3  
4  
5  
6  
7  
8  
9  
10  
11  
12  
13  
14  
15  
16  
17  
18  
19  
20  
21  
22  
23  
24  
25  
26  
27  
28  
29  
30  
31  
32  
33  
34  
35  
36  
37  
38  
39  
40  
41  
42  
43  
44  
45  
46  
47  
48  
49  
50  
51  
52  
53  
54  
55  
56  
57  
58  
59  
60  
61  
62  
63  
64  
65

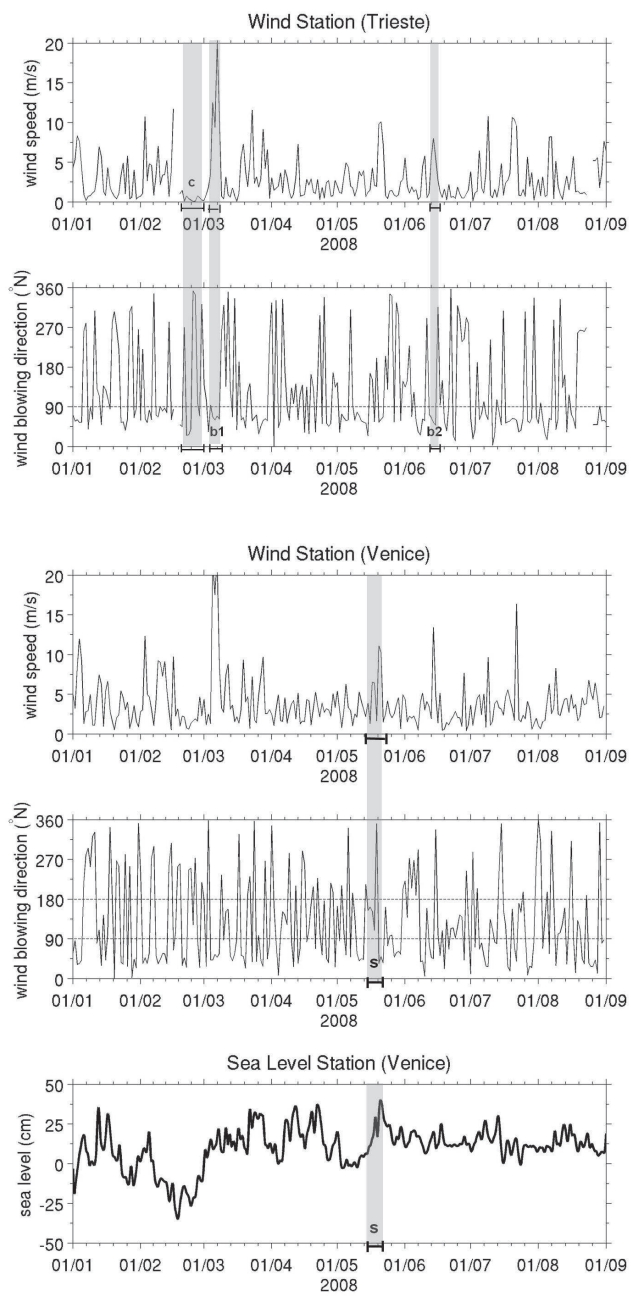


Figure 2: The wind periods selected: in the two upper panels the calm wind period (c) and the two Bora episodes (strongest b1 and weaker b2) from the wind time series in Trieste. The two panels in the middle indicate the Sirocco episode (s) identified from the wind time series in Venice. The lowest panel represents the sea level time series in Venice station with the selected Sirocco event (s).

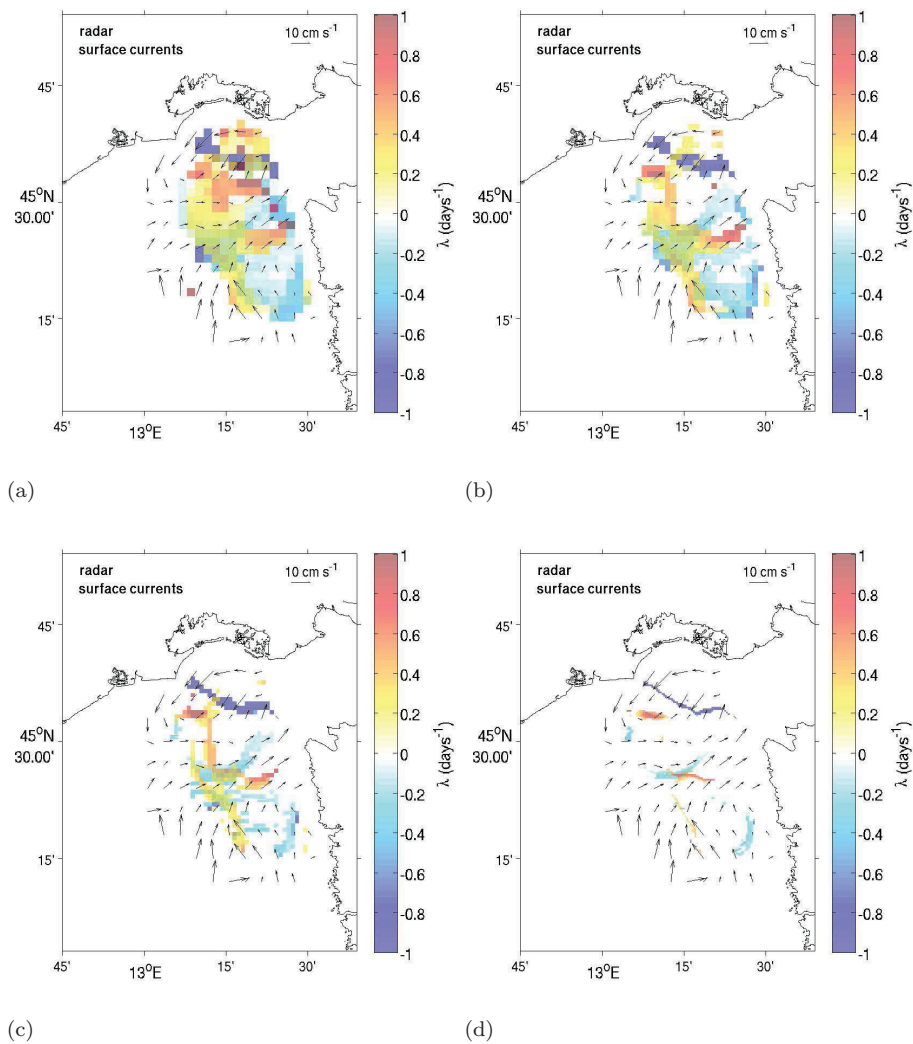


Figure 3: FSLE ( $\text{days}^{-1}$ ) trial maps for different  $\delta_i$ : (a) 2 km, (b) 1.4 km, (c) 1 km and (d) 0.4 km. The parameter  $\delta_f$  is set to 3 km. Black arrows indicate the surface currents configuration at the beginning of the trajectories simulation. The radar current field has been sub-sampled (one vector every five grid nodes) for graphical readability.

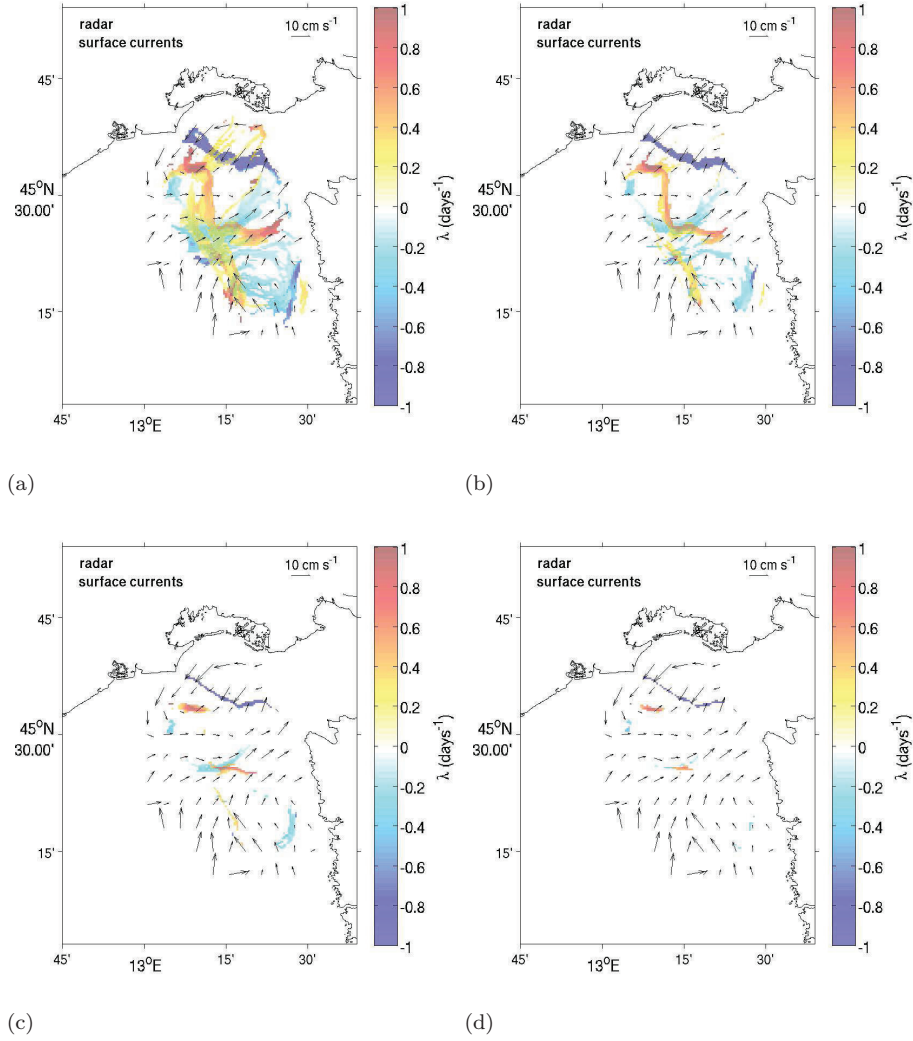


Figure 4: FSLE ( $\text{days}^{-1}$ ) trial maps for different  $\delta_f$ : (a)1 km, (b)1.6 km, (c)3 km and (d)5 km. The parameter  $\delta_i$  is set to 0.4 km. Black arrows indicate the surface currents configuration at the beginning of the trajectories simulation. The radar current field has been sub-sampled (one vector every five grid nodes) for graphical readability.

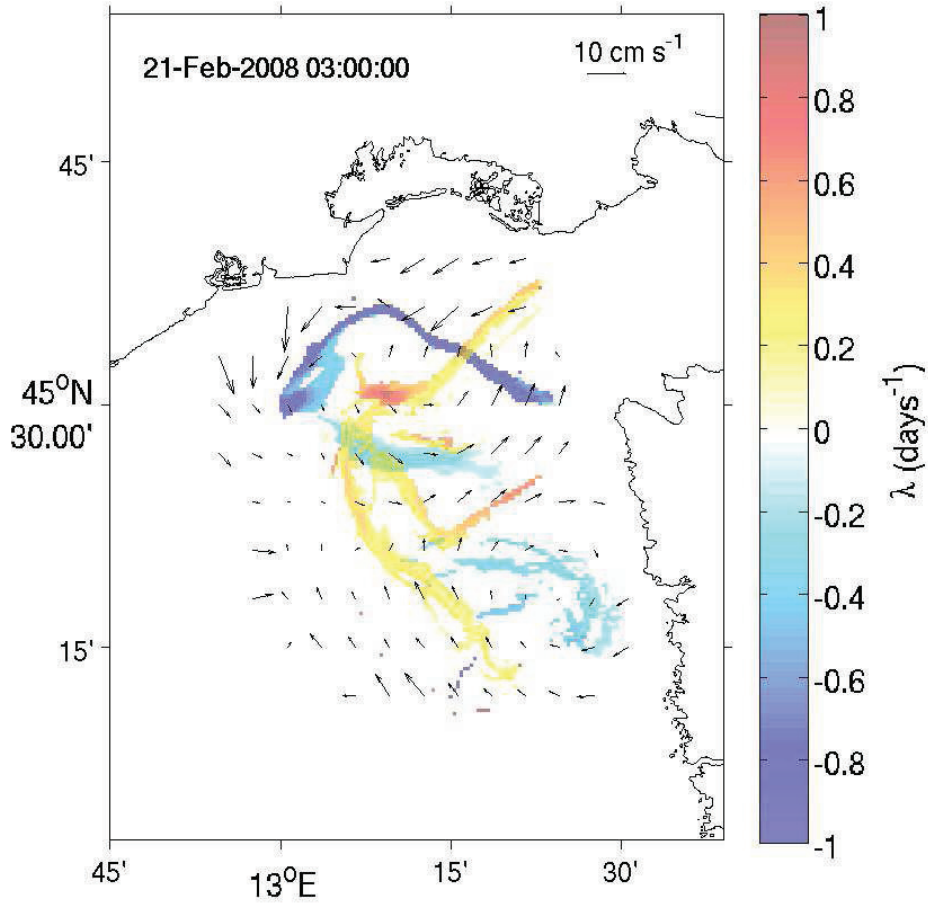
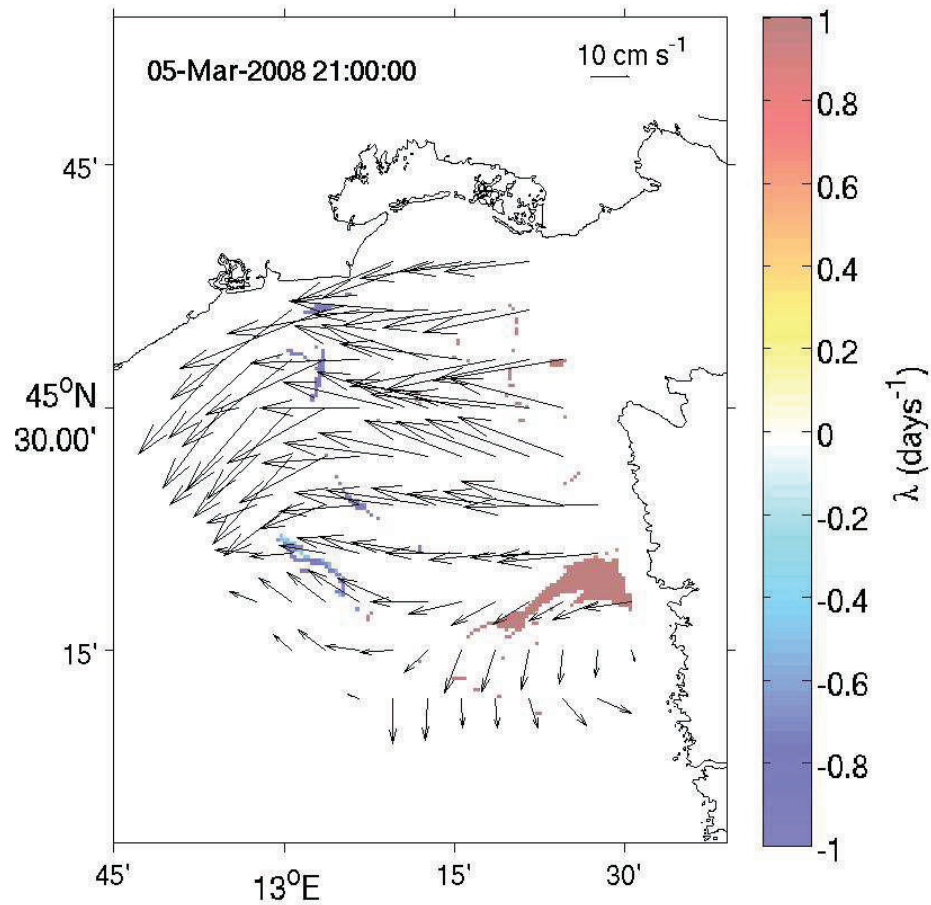
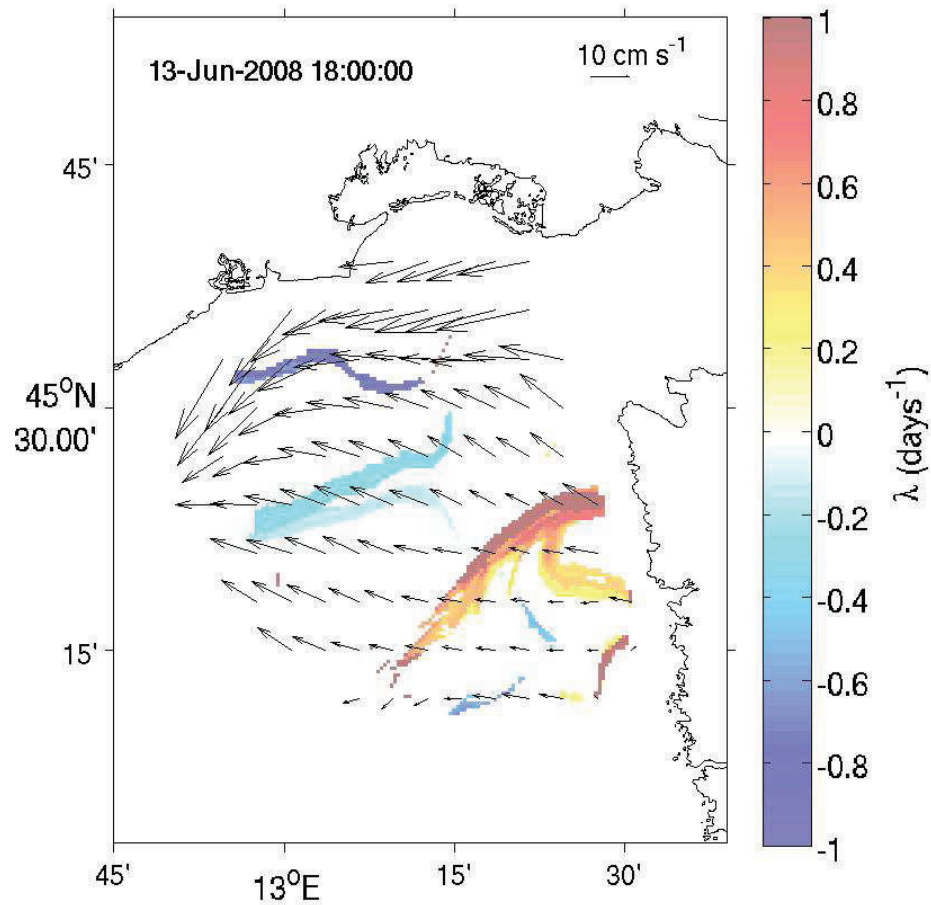


Figure 5: FSLE ( $\text{days}^{-1}$ ) map extracted from the calm wind period in February 2008. Black arrows indicate the mean surface current field during the calm wind period. The date specifies the beginning of the trajectories simulation. The radar current field has been sub-sampled (one vector every five grid nodes) for graphical readability.



(a)



(b)

Figure 6: FSLE (days<sup>-1</sup>) maps extracted from the Bora episodes: (a) in March 2008 and (b) in June 2008. Black arrows indicate the mean surface current field during the wind episode. The date specifies the beginning of the trajectories simulation. The radar current field has been sub-sampled (one vector every five grid nodes) for graphical readability.



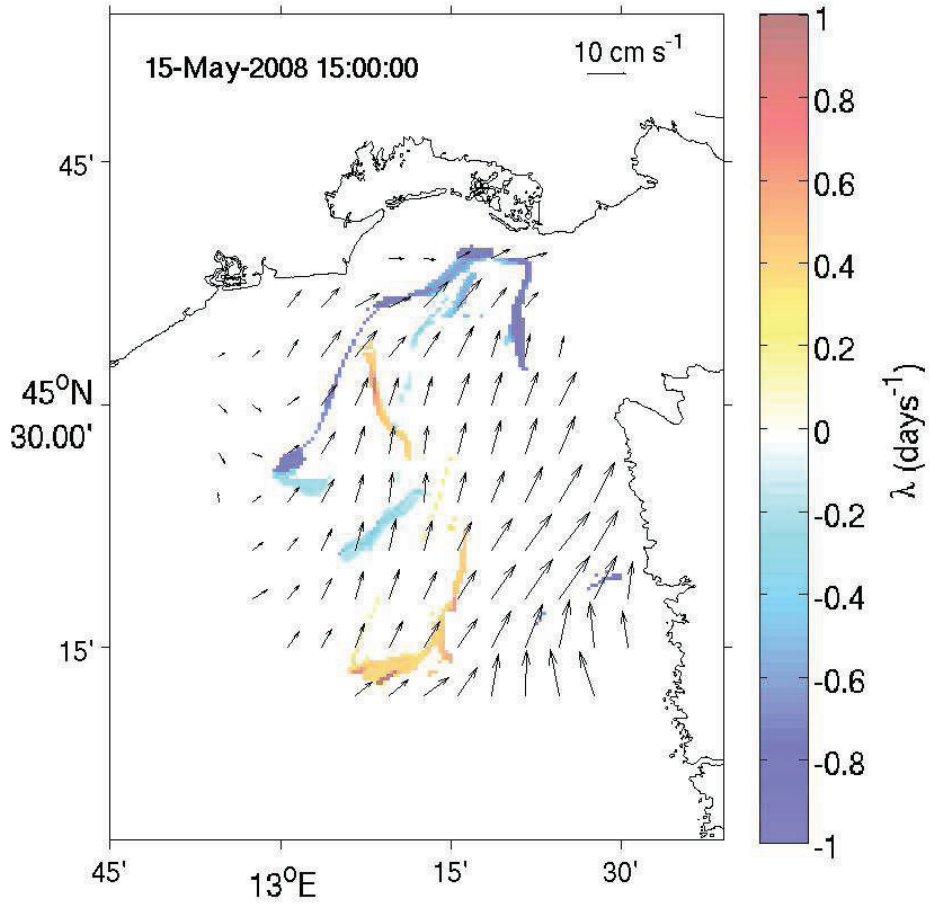


Figure 7: FSLE (days<sup>-1</sup>) map extracted from the Sirocco episode in May 2008. Black arrows indicate the mean surface current field during the wind episode. The date specifies the beginning of the trajectories simulation. The radar current field has been sub-sampled (one vector every five grid nodes) for graphical readability.